表1　レビー小体型認知症(DLB)診断基準改訂版

1：中心的特徴(診断に必須)
　認知症(正常な社会的・職業的機能に支障をきたすほどの進行性認知低下)
　早い時期には著明な，または持続性の記憶障害は必ずしも起こらなくてもよいが，通常は進行とともに明らかになる
　注意や実行機能や視空間能力のテストでの障害が特に目立つこともある
2：コア特徴(probable DLBの診断には2つ，possible DLBの診断には1つ)
　1)注意や明晰性の著明な変化を伴う認知の変動
　2)典型的には構築された具体的な繰り返される幻視
　3)特発性のパーキンソニズム
3：示唆的特徴(1つ以上のコア特徴があり，1つ以上の以下の特徴があれば，probable DLBの診断が可能．コア特徴がなくても，1つ以上の示唆的特徴があればpossible DLBの診断には十分．Probable DLBは示唆的特徴だけでは診断するべきではない)
　1)レム睡眠行動異常
　2)重篤な抗精神病薬への過敏性
　3)SPECTまたはPETで示される基底核でのドパミントランスポーターの取り込み低下
4：支持的特徴(普通はあるが，診断的特異性は証明されていない)
　繰り返す転倒や失神
　一過性の説明困難な意識消失
　重篤な自立神経障害：たとえば，起立性低血圧，尿失禁
　他の幻覚
　系統的な妄想
　抑うつ
　CT/MRIでの内側側頭葉の比較的保持
　SPECT/PETでの後頭葉低活性を伴う全般性低活性
　MIBG心筋シンチグラフィーでの取り込み低下
　脳波での側頭葉の一過性鋭波を伴う目立った徐波化
5：DLBの診断の可能性が乏しい
　局所性神経徴候や脳画像でみられる脳血管障害の存在時
　部分的あるいは全般的に臨床像を説明しうる他の身体疾患または脳疾患の存在時
　重篤な認知症の時期にはじめてパーキンソニズムが出現した場合

(文献[6]より引用)

かはっきりしない．診断はいわゆる「1年ルール」にのっとると，認知症を伴うパーキンソン病が考えられるが，臨床的にはこれをDLBと厳密に区別する意義は乏しいとされる[6]．本症例はDLB診断基準改訂版(表1)の，中心的特徴である進行性の認知機能低下に加え，中核的特徴である認知の変動，具体的な繰り返される幻視，特発性のパーキンソニズムの3つを認めたため，probable DLBと診断し，問題となる症状への対応を重視した．

症例2は，30代で出産した後は，1年間をうつ病期，軽躁期および寛解期でちょうど3等分しているかのようにみえた．こうした活動性の変化をみる限り躁うつ病圏の疾患が考えやすい．しかし，経年とともに「寝込む時期」，つまりうつ病相らしき時期が長引くようになり，初老期には被害関係妄想が出現している．この経過を振り返ると，古茶が遅発性緊張病について，症候学的特徴，病像の推移および経過について詳細にまとめている[7]が，患者は年に1回の周期で訪れる初期抑うつ期をどうにか乗り切っていたが，徐々に不安・焦燥期に移行してそれが困難になってしまったのではないであろうか．初回入院への強い抵抗は，その時期の強い不安・焦燥を表しているのであろう．その後連続して幻覚妄想期に至り，近所の人物を対象として妄想を抱いたため精神科初診時には妄想性障害との診断がなされ，抗精神病薬での治療が必要となったのであろう．

その後どちらの症例も(亜)昏迷，筋固縮，姿勢保持等の症状から緊張病症候群と判断された．身体疾患の治療後も改善しない発熱が持続することより，悪性緊張病の可能性も検討されたが，経過を通じて血圧や脈拍などはほぼ正常と自律

神経系は安定していた．

緊張病症候群の治療としては薬物療法としてはBZ系が第1選択薬とされる[1]．Rosebushらが緊張病症候群の急性期に対してlorazepamの効果を調べた試験によると，15例の急性期緊張病エピソードに対し同薬を1～2 mg投与したところ，2時間以内に12例(80%)で劇的に症状が消失したという[8]．本邦では長岡ら[9]，当科でも藤原ら[10]が緊張病症状を呈したDLBにBZ系を投与した症例について報告しているが，症例1のようにDLBである場合，認知機能への影響やBPSDの悪化等が危惧されるためBZ系の投与は慎重にならざるを得ない．今回の症例1では日中の睡眠覚醒リズムの障害を招いたため投与を断念した．しかし，当科の他の症例ではlorazepamが効果的と考えられたものもある．投与においては，単純にDLBに不利益と決めつけずベネフィットとリスクを慎重に検討することが重要であろう．

緊張病症候群に対するもう1つの治療としてmECTがあげられる．Finkは著書の中で，カタトニアの治療において薬物治療が失敗したらECTの出番であると述べている[2]．症例1はDLBと診断しているが，当科に転院直後から緊張病症候群を呈していることを考慮し，抗認知症薬ではなくBZ系での治療を優先し，その後にmECTを導入した．また，FinkはBZチャレンジテストについても述べている[2]が，症例2ではdiazepamへの反応は良好であったにもかかわらず，内服のlorazepamへの反応は期待したものとは異なり，興奮や幻視が前景に立つようになった．そのため，早急な症状の改善を期待し，mECTへ移行する方針とした．両症例とも，mECTを施行する際には，各セッションの波形の評価において，上田が述べているような評価項目を用いて評価し[11]，次回の刺激強度の決定の参考にした[12]．

その効果について振り返ると，両症例とも第1セッション当日の施行後から両上肢の筋固縮が改善し自発的運動も認められるなど，四肢の運動障害は著明な改善が認められた．昏迷からも脱し発語量も増えるなど意欲面での改善も認められた．解熱傾向となり誤嚥性肺炎も認めなくなった．精神症状に関しては幻視が減少し妄想や興奮も消失した．DLBの診断基準のうちの支持的特徴としてSPECTでの後頭葉の血流低下があるが[56]，これが幻視や視覚認知障害との関連が考えられている．矢野らの報告では，幻視，抑うつ，昏迷を呈したDLB症例で，mECT後にSPECTにおいて後頭葉の血流低下の改善を認めている[13]が，症例1でも類似した所見が認められる．前述のとおり症例1は血流低下の程度が軽度であり幻視の原因と断定するのは困難であるが，仮に，幻視の原因となるような局所的な血流低下をmECTにより改善できるとすれば，臨床症状およびSPECTの局所的な血流低下とも典型的な所見の場合，mECTの効果はある程度予測可能となるかもしれない．

## おわりに

緊張病症候群を呈した2例を経験した．緊張病症候群に至るまでの経過は大きく異なっていたが，いずれも筋固縮，昏迷，発熱といった症状を認めた．治療反応性という観点においては，BZ(benzodiazepine)系に対する反応は異なっていたが，mECTには両者とも良好な反応を示した．レビー小体型認知症(dementia with Lewy bodies；DLB)と遅発緊張病という類似しながらも異なる部分もある疾患の2例であったが，実臨床においては緊張病症候群への治療を適切に行うことの重要性を再確認した．精神疾患で緊張病症状を認めた場合，操作的診断基準に従えば異なる診断とされる疾患においても緊張病症候群として新たな診断の亜型を提案することが可能ではないかと示唆される2症例であった．

## 文　献

1) 大久保善郎．カタトニア(緊張病)症候群の診断と治療．精神経誌 2010；112：396.
2) Fink M, Taylor MA. Catatonia : A Clinician's Guide to Diagnosis and Treatment. Cambridge : Cambridge University Press ; 2003.〔鈴木一正・訳．カタトニア．臨床医のための診断・治療ガイドライン．東京：星和書店；2007.〕
3) Taylor MA, Fink M. Catatonia in psychiatric classification : a home of its own. Am J Psychiatry 2003 ; 160 : 1233.
4) 小阪憲司．DLBの初期診断．Mod Physician 2006；

26：1869.
5) Nagahama Y, Okina Y, Suzuki N, Matsuda M. Neural correlates of psychotic symptoms in dementia with Lewy bodies. Brain 2010 ; 133 : 557.
6) McKeith IG, Dickson DW, Lowe J, et al. Diagnosis and management of dementia with Lewy bodies : Third report of the DLB consortium. Neurology 2005 ; 65 : 1863.
7) 古茶大樹．遅発緊張病について．日本生物学的精神医学会誌 2010；21：3.
8) Rosebuch PI, Hildebrand AM, Furlong BG, et al. Catatonic syndrome in a general psychiatric inpatient population : frequency, clinical presentation, and response to lorazepam. J Clin Psychiatry 1990 ; 51 : 357.
9) 長岡研太郎，橋本　衛，大川愼吾．レビー小体病に生じた緊張病症候群にlorazepamが奏功した2症例．精神科治療学 2004；19：1259.
10) 藤原(大橋)愛子，久保達哉，杉本　流，ほか．自殺企図を呈し入院に至ったレビー小体型認知症の1例～その問題点と考察～．九神精医 2012；58：83.
11) 上田　諭．電気けいれん療法のエビデンス―施行方法が効果と安全性を決める―．老年精神医学雑誌 2013；24：471.
12) 上田　諭．発作脳波の有効性判定と1.5倍の刺激%上げ幅が必須―パルス波ECT施行の前提と倫理―．臨床精神医学 2013；42：421.
13) 矢野智宣，小野陽一，森　秀徳，ほか．m-ECTにより後頭葉の著明な血流改善を認めたDLBの1例．臨床精神医学 2006；35：1269.

*　　*　　*

Pediatric Neurology 50 (2014) 31–37

Contents lists available at ScienceDirect

Pediatric Neurology

journal homepage: www.elsevier.com/locate/pnu

Original Article

# Corticosteroid Therapy for Duchenne Muscular Dystrophy: Improvement of Psychomotor Function

**Yuko Sato PhD [a,b], Akemi Yamauchi MD, PhD [b], Mari Urano MA [b], Eri Kondo MD [b], Kayoko Saito MD, PhD [a,b,*]**

[a] *Affiliated Field of Genetic Medicine, Division of Biomedical Engineering and Science, Graduate Course of Medicine, Graduate School of Tokyo Women's Medical University, Tokyo, Japan*
[b] *Institute of Medical Genetics, Tokyo Women's Medical University, Tokyo, Japan*

ABSTRACT

**BACKGROUND:** Of the numerous clinical trials for Duchenne muscular dystrophy, only the corticosteroid prednisolone has shown potential for temporal improvement in motor ability. In this study, the effects of prednisolone on intellectual ability are examined in 29 cases of Duchenne muscular dystrophy because little information has been reported. And also, motor functions and cardiac functions were evaluated. **METHODS:** The treated group was administered prednisolone (0.75 mg/kg) orally on alternate days and the compared with the untreated control group. Gene mutations were investigated. The patients were examined for intelligence quotient adequate for age, brain natriuretic peptide, creatine kinase, and manual muscle testing before treatment and after the period 6 months to 2 years. **RESULTS:** Intelligence quotient scores of the treated increased to 6.5 ± 11.9 (mean ± standard deviation) were compared with the controls 2.1 ± 4.9 ($P = 0.009$). Intelligence quotient scores of the patients with nonsense point mutations improved significantly (21.0 ± 7.9) more than those with deletion or duplication (1.9 ± 9.0; $P = 0.015$). Motor function, such as time to stand up, of those treated improved significantly and brain natriuretic peptide level was reduced to a normal level after treatment in 15 patients (73%). **CONCLUSIONS:** Our results demonstrate the effectiveness of prednisolone in improving intellectual impairment as well as in preserving motor function and brain natriuretic peptide levels. We presume that prednisolone has a read-through effect on the stop codons in the central nervous systems of Duchenne muscular dystrophy because intelligence quotient of point mutation case was improved significantly.

***Keywords:*** Duchenne muscular dystrophy, prednisolone, cognition, motor function

Pediatr Neurol 2014; 50: 31-37



## Introduction

Duchenne muscular dystrophy (DMD) is the most common type of childhood muscular dystrophy. It is characterized by progressive muscle weakness and deterioration of skeletal and cardiac muscle function. DMD is an X-linked recessive disorder, caused by mutations in the *DMD* gene in Xp21.1, leading to complete absence of the cytoskeletal protein dystrophin in both skeletal and cardiac muscle cells.[1] Several treatments involving drugs with read-through effects have attracted major interest, such as the amino glycoside antibiotic gentamicin[2,3] and PTC124[4] as well as antisense morpholinos that cause exon skipping.[5] These treatments are, however, being administered only as clinical research regimens at present and have not yet reached the stage of extensive clinical application. The only widely used clinically effective treatment for DMD patients is oral administration of prednisolone (PSL). This treatment was highly evaluated, as evidence level 1, by the US Neurology Academy and at the US Pediatric Neurology Meeting in 2005.[6]

PSL is believed to temporarily slow motor function decline and disease progression. In our daily examination of

*Article History:*
Received March 20, 2013; Accepted in final form July 31, 2013

* Communications should be addressed to: Dr. Saito; Director and Professor, Institute of Medical Genetics; Tokyo Women's Medical University; 10-22 kawada-cho; shinjyuku-ku; Tokyo 162-0054, Japan.
*E-mail address:* saito@img.twmu.ac.jp

0887-8994/$ - see front matter © 2014 Elsevier Inc. All rights reserved.
http://dx.doi.org/10.1016/j.pediatrneurol.2013.07.022

**TABLE.**
Comparison of two groups before PSL

| | Treated Group (n = 20)* | Control Group (n = 9)* | *t* Test ($P < 0.05$) |
|---|---|---|---|
| Age at treatment onset (yr) | 5.9 ± 0.2 | 6.1 ± 0.6 | $P = 0.7099$ |
| Time required to stand before PSL (seconds) | 3.9 ± 0.3 | 4.6 ± 4.8 | $P = 0.5711$ |
| Gluteus maximus muscle strength before PSL | 3.4 ± 0.1 | 3.4 ± 0.2 | $P = 0.2250$ |
| Iliopsoas muscle strength before PSL | 3.4 ± 0.1 | 3.5 ± 0.3 | $P = 0.0944$ |
| CK (IU/L) before PSL | 15,492 ± 1662 | 14,414 ± 1091 | $P = 0.3317$ |

Abbreviations:
CK = Creatine kinase
PSL = Prednisolone
SE = Standard error
* Mean ± SE.

patients, we recognized that PSL administration improves responsiveness, verbal rapport, and motor functions in DMD patients. Thus, we hypothesized that PSL also has an ameliorating effect on central nervous system dysfunctions, including intellectual impairments.

In this study, we measured intelligence quotients (IQs) to evaluate intellectual abilities before and from 6 months to 2 years after starting PSL administration. We used the Stanford-Binet Intelligence Test (5th edition), which is the standardized version of the Stanford-Binet method applied in Japan for evaluating preschool children and the Wechsler Intelligence Scale for Children, 3rd edition, which is used in school-age children.

For motor function, we also measured the time required to stand up and lower limb strength using manual muscle testing. We measured serum creatine kinase (CK) titers to assess the state of skeletal muscles.

Furthermore, because 50% of DMD patients develop heart failure resulting from left cardiac dysfunction,[7] plasma brain natriuretic peptide (BNP) levels were also measured to evaluate cardiac muscle function. BNP served as a marker of cardiac function in the treated group. BNP is known to be an adequately sensitive marker for detection of stage 1 heart failure. Furthermore, Sakurai et al reported correlations between plasma BNP level and indices of cardiac function.[8]

## Materials and Methods

*Identification of genetic mutations*

Mutations were investigated in all patients to detect deletion or duplication of genes by multiplex polymerase chain reaction or multiplex ligation-dependent probe amplification using a Holland P034/P035 DMD kit (FALCO Biosystems). In patients in whom neither method revealed any abnormalities, point mutation analyses employing complementary DNA direct sequencing were performed with messenger RNA extracted from peripheral blood lymphocytes or biopsied muscle tissues.

*Clinical analyses before and after PSL administration*

Twenty-nine DMD patients were divided into a treated group and a control group. The 21 patients in the treated group (mean age: 5.9 years) were outpatients between 1994 and 2010 at the Department of Pediatrics, or the Institute of Medical Genetics of Tokyo Women's Medical University. PSL (0.75 mg/kg) was orally administered on alternate days.[9–11] The other eight patients, all with identified gene mutations, comprised the control group (mean age: 6.1 years). The other eight patients had been followed at the Department of Pediatrics between 1980 and 1990 and had detailed medical records available (Table).

*Investigation of IQ scores*

IQ scores were examined before PSL administration and also 6 months to 2 years after starting PSL. IQ scores are numerical values that express the results of an intelligence test. A score of 80 or above is considered to be within normal range, whereas a score between 70 and 79 is borderline, 50 to 69 indicates mild intellectual impairment, 35 to 49 indicates moderate intellectual impairment, and 35 or below is classified as severe intellectual impairment.[12] Subjects were divided into three groups based on the degree of IQ score changes, namely, an increase group, in which IQ scores increased by 10 or more points; an unchanged group, in which IQ score changes were within 0 to 10 points; and a decrease group, in which IQ scores dropped by 10 or more points after PSL administration.

The IQ testing method was selected according to the age and developmental stage of each subject. The IQ testing methods differ before and after school age. In preschool children, IQ might be measured by WPSSI (Wechsler Preschool and Primary Scale of Intelligence). In Japan, however, the WPSSI-IV is not as yet a standard test, whereas the WPSSI-III was in use for 30 years, although it would not now be considered appropriate. Therefore, a standardized version of the Stanford-Binet method has been adopted for preschool children. For school-age children, IQ should be measured employing the Wechsler Intelligence Scale for Children, 3rd edition, which is used to evaluate and measure both performance and verbal IQ. We adopted the Japanese version of Wechsler Intelligence Scale for Children, 3rd edition, for school-age children in this study.

*Measurement of motor functions and CK and BNP levels before and after PSL administration*

The effects of PSL were observed by measuring motor functions, including the time required to stand up and muscle strength by manual muscle testing, to compare the treated and control groups. Furthermore, because 50% of DMD patients develop heart failure resulting from left cardiac dysfunction, BNP levels were measured in the treated group to allow comparison of cardiac functions among genetic mutation types.

*Time required to stand up.* The time required to stand up from a supine to a standing position was measured in 18 patients in the treated group and eight in the control group.

*Muscle strength.* Muscle strength was measured in 16 of the treated patients and in the eight control group patients who had periodically undergone manual muscle testing. Because DMD is characterized by proximal muscle weakness, the strength of the gluteus maximus and iliopsoas muscles were measured under conditions of both supine hip flexion and prone hip extension. The strength of the gluteus maximus and iliopsoas muscles were also investigated. All physical examinations, including the manual muscle testing, were conducted by the same doctor.

*CK levels.* Levels of CK, the skeletal muscle enzyme, were measured in 15 of the treated patients and in the eight control patients, with values of

200 IU/L or less being considered normal. CK titers were studied at regular visits to our institute. The activity levels on the day of measurement and the previous day were not taken into consideration.

*BNP levels.* BNP levels were measured in 15 of the 21 treated patients, with 18 pg/mL or less being considered normal. BNP is known to be an adequately sensitive marker to detect heart failure at stage 1, when clinical symptoms are not yet apparent. Sakurai et al (2003) reported the plasma BNP level to correlate with indices of cardiac function. No patients in the treated group were taking parasympathetic agents, adenosine receptor modulating drugs, or angiotensin-converting enzyme inhibitors, all of which can affect cardiac function. BNP levels and gene mutilation types were compared.

This study was approved by the Ethics Committee of Tokyo Women's Medical University (no. 2116).

## Results

*Identification of genetic mutations*

Of the29 study participants undergoing genetic analysis, nonsense point mutations were identified in five (control group 0; treated group 5), exon deletions in 22 (control group 8; treated group 14), and exon duplications in 2 (control group 0; treated group 2).

*Clinical and biochemical analyses before and after PSL administration*

*Investigation of IQ scores*

The IQ level had increased significantly in the treated group 6 months to 2 years after starting treatment, as compared with the control group. IQ scores of the treated group were thus increased by 6.5 ± 11.9 points (mean ± SD) as compared with those of the controls (2.1 ± 4.9) ($P = 0.009$) (Fig 1A, B). Differences among the three genetic mutation types were also compared and the IQ scores of patients with nonsense point mutations were increased 21.0 ± 7.9 points, showing a greater improvement than those with deletion or duplication mutations (1.9 ± 9.0) ($P = 0.015$) (Fig 1C, D).

*Measurements of motor functions and CK and BNP levels*

*Time required to stand up.* The time required to stand up in the control group was 5.7 ± 1.3 seconds (mean ± SD), showing a

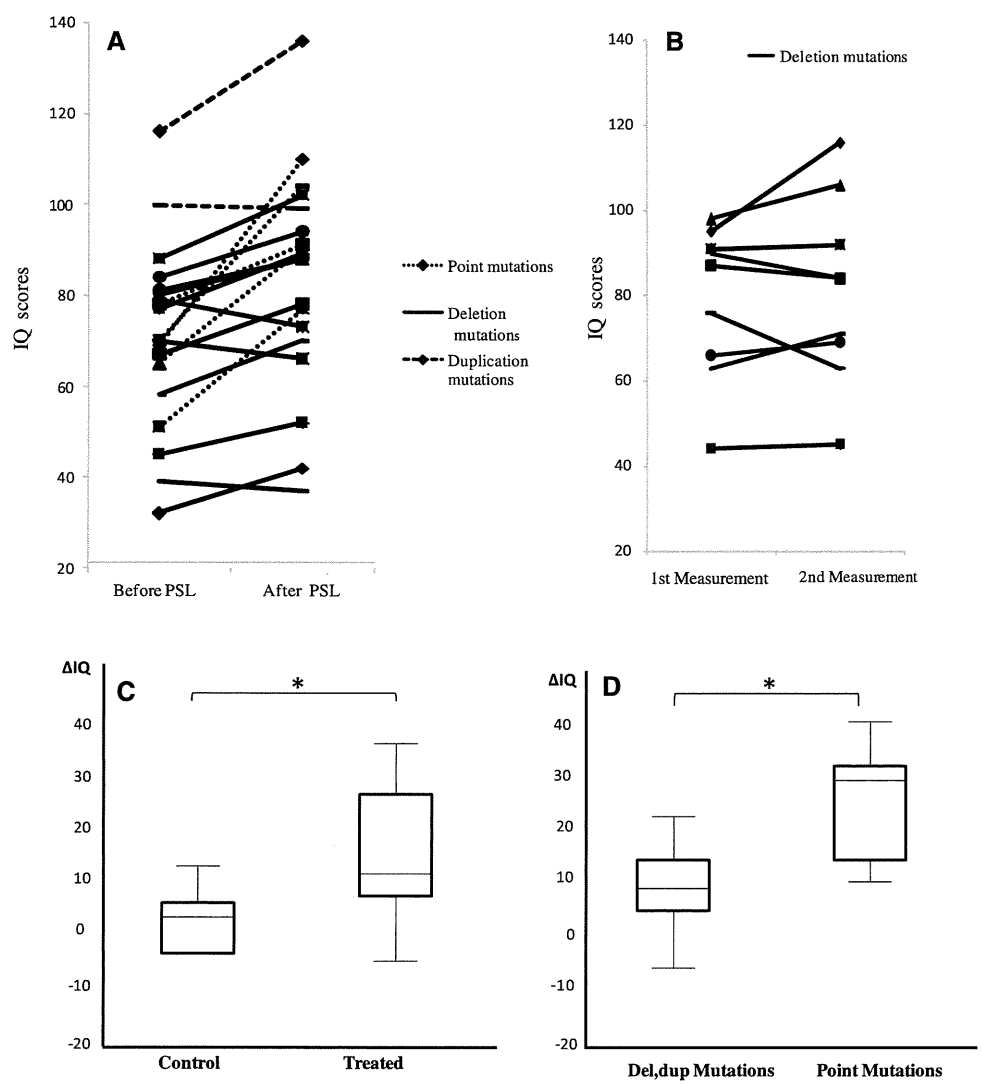


**FIGURE 1.**
Investigation of IQ scores after PSL. (A) IQ scores of treated group; (B) IQ score of control group; (C) ΔIQ scores compared between the above two groups (P=0.009); (D) ΔIQ scores compared between nonsense point mutation and a group of deletion + duplication (P=0.0015).

marked increase over time, whereas that of the treated group was 3.3 ± 0.2 seconds and was thus unchanged 6 months to 2 years after the start of PSL treatment ($P = 0.031$) (Fig 2A).

*Muscle strength.* The strengths of the gluteus maximus and iliopsoas muscles were investigated for 6 months to 2 years. Gluteus maximus muscle strength differed significantly between the two groups after 2 years. Iliopsoas muscle strength was at 3.5 ± 0.9 (mean ± SD) in the treated group, whereas it decreased to 3.1 ± 0.2 in the control group ($P = 0.048$) (Fig 2B). However, the difference between the two groups did not reach statistical significance ($P = 0.222$).

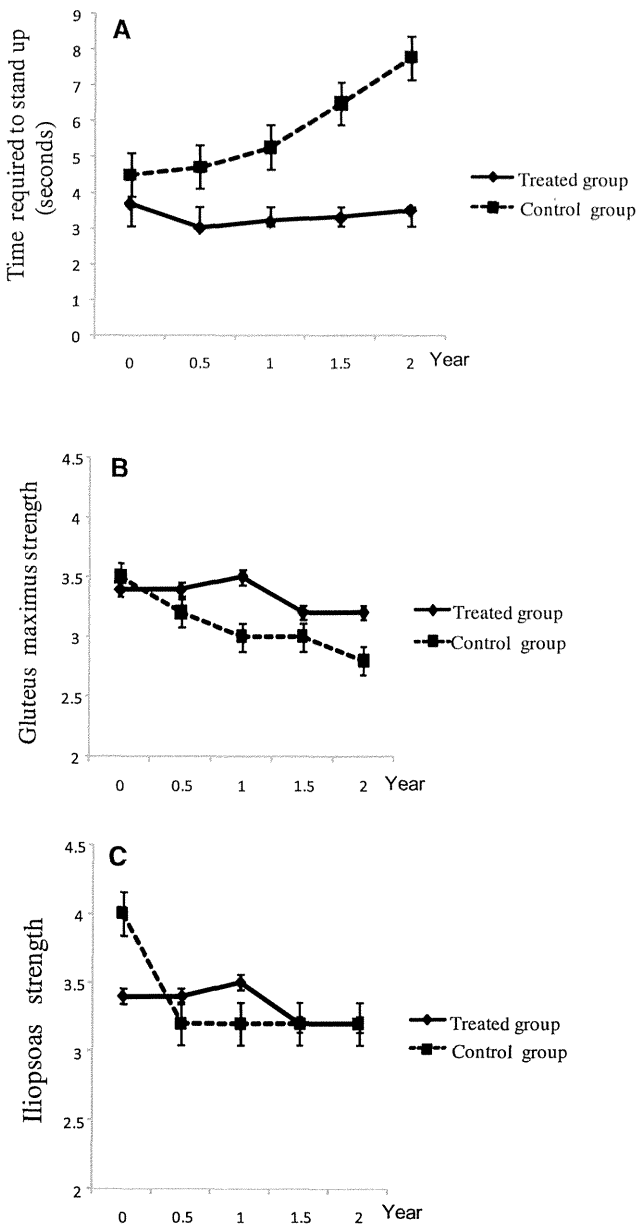


**FIGURE 2.**
Evaluation of the muscular power after PSL. (A) The times required to stand up between treated and control groups (P=0.031); (B) The strength of the Gluteus maximus muscle by MMT between 2 groups (P=0.048); (C) Iliopsoas muscle strength by MMT between two groups (P=0.222).

*CK levels.* The patients had high CK levels, which is common for pediatric DMD patients at the onset of treatment. However, these levels did not change significantly over the course of treatment and there was no significant difference between the two groups at the end of follow-up ($P = 0.505$) (data not shown).

*BNP levels.* After PSL administration, the BNP levels of 15 patients (73%) in the treated group were normal. Of those 15 patients, four had nonsense point mutations, nine had deletion mutations, and two had duplication mutations. BNP was significantly lower at 5.1 ± 4.0 (mean ± SD) in patients with point mutations 1 year after the start of PSL administration than the level of 7.7 ± 5.5 in those with deletion and duplication type mutations ($P = 0.034$) (Fig 3).

## Discussion

DMD patients are generally diagnosed at 2-3 years of age. There is a steady decline in motor function after age 6. By age 10, braces may be required for walking, and by age 12, patients are confined to a wheelchair. Most are bedridden by approximately age 15. A few individuals with DMD who live beyond their 30s require artificial ventilation because of diaphragm muscle failure. Intellectual abilities vary widely among DMD patients. Although some have normal intellectual abilities, others exhibit intellectual impairments. A few patients do not even attain meaningful words. Others also have developmental disabilities such as autistic spectrum disorders or attention deficit hyperactivity disorders. Many studies on the IQ scores of DMD patients have already been published.[12] The mean IQ score among these reports was reported as 82. Until the 1950s, the intellectual disability observed in some DMD patients was attributed to secondary effects of motor disability and muscle weakness, namely physical and social barriers in addition to the lack of educational opportunities.[13] It was subsequently recognized that intellectual impairment is present before the appearance of the symptoms of muscle weakness and atrophy. Intellectual impairment was found to be nonprogressive and there were no correlations among IQ scores, age, and disease progression.[14-16] There is, at present, no evidence supporting the concept that intellectual impairment in DMD patients is a secondary effect of muscle weakness. Intellectual impairment is now considered to be caused by genetically determined dysfunctions impacting the central nervous system.

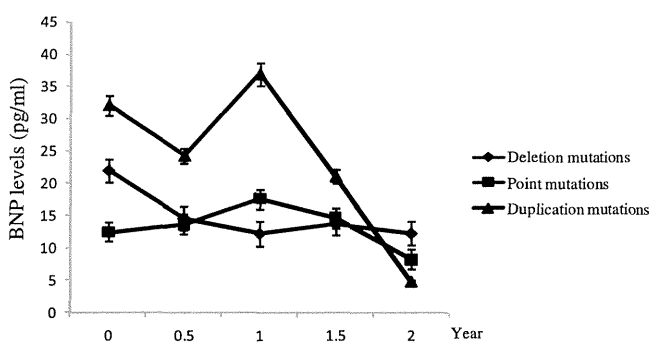


**FIGURE 3.**
Transition of BNP levels after PSL treatment among 3 gene mutation groups; the lowest in nonsense point mutation.

When PSL treatment for DMD patients was started, the daily dosage was high at 2 mg/kg/day. As a result, various adverse reactions were observed, such as cushingoid facial features, weight gain, and behavioral abnormalities. Thereafter, the establishment of appropriate doses was investigated by comparing side effects at PSL doses of 1.5, 0.75, and 0.3 mg/kg/day administered daily for 6 months by a consortium on muscular dystrophy.[9] In the present study, the selected PSL dose was administered as an alternate-day medication regimen of 0.75 mg/kg/day.[17] Converted into a daily dose, this would be within a daily medication range of 0.12-0.5 mg/kg/day, which is a commonly prescribed amount. Efficacy not inferior to that of a daily medication regimen is provided, with the major advantage of avoiding adverse reactions.

*Evaluation of intellectual ability before and after PSL administration*

Along with physical problems, mental problems have been recognized in association with DMD. It has been estimated that approximately one third of DMD patients suffer from mental retardation or other forms of intellectual impairment. The IQs of DMD patients are reportedly in the range of 68-91, with the average being in the mid-80s. Characteristically, verbal IQ has been somewhat better than performance IQ.[18]

Intellectual impairment does not appear to progress as motor function deteriorates.[19,20] In this study, the mean IQ score of our 29 patients was 85, which is consistent with previous reports. Also, IQ scores generally remain constant. Although slight fluctuations may occur because of environmental factors, changes exceeding 10 points are considered rare.[21] This was also supported by the observations of our control group in which IQ scores did not change. However, when we started PSL treatment, improvements in verbal rapport and reactions were clearly recognized clinically in several patients, leading us to hypothesize that PSL had exerted a beneficial influence on intelligence.

In this study, the maximum IQ score increase was 23 points in a treated patient, which is an extraordinary improvement (Fig 1A). IQ scores were increased as compared with those of the control group ($P = 0.009$) (Fig 1C).

No previous studies, to our knowledge, have examined the effects of PSL on intellectual ability in pediatric patients. For adult patients, effects of PSL on the central nervous system are suggested to represent modulations of neurological symptoms such as mood disorders including depression and mania, psychiatric disorders such as delirium and hallucinations, and cognitive or memory impairments. There are several possible mechanisms by which PSL might exert such effects on neurological symptoms. One possibility is the strong affinity of PSL for receptors, particularly those of the limbic system including the hippocampus, all because PSL may affect the activities of regional neurotransmitters. Other possible mechanisms include involvement of central synapses in prolonged neurotransmission latency periods associated with changes in blood-brain barrier permeability and impairments of cerebral metabolic enzymes. Any or all of these factors might be mechanisms underlying neurological symptom onset.[22] However, none of these neurological symptoms was found in our DMD patients. Instead, improvements of verbal rapport, reactions, and IQ scores were observed. Thus, we hypothesized that PSL acts differentially on the central nervous system in DMD patients.

Symptoms of DMD are accounted for by lack of dystrophin protein. Dystrophin is mostly expressed in muscles, with the next highest level of expression being in the brain.[23] Intracranial dystrophin is known as cerebral dystrophin and exists in the postsynaptic membrane, which is a neurotransmitter circuit.[24]

If PSL accelerates muscular dystrophin production, cerebral dystrophin would also be increased, thereby ameliorating intellectual impairment. Cerebral dystrophin comprises various isoforms produced from one gene, and the isoforms exist in the postsynaptic membrane, which is a neurotransmitter circuit. Because various isoforms of dystrophin exist in neurons in the central nervous system, it is possible that mutation of the DMD gene would result in dysfunction of neurons, thereby influencing not only intellectual levels but also determining specific neuropsychological profiles. However, there is still a great deal of uncertainty regarding the roles played by these various isoforms.[25]

An experiment with mdx mice demonstrated that cerebral dystrophin was extensively distributed throughout the hippocampus, which is chiefly related to memory, the cerebellum, and the olfactory bulbs, governing sensation and motor function, and the thalamus, which has important roles in activity and consciousness levels.[26]

It has also been reported that abnormalities of cerebral dystrophin isoform formation can cause central nervous system structural anomalies, dendritic cell defects, and decreased numbers of neurons.[27] This suggests that cerebral dystrophin anomalies resulting from abnormal brain isoform formation might be the primary cause of intellectual impairment. If PSL promotes the formation of dystrophin expressed in muscle cells, it must also activate production of cerebral dystrophin in the central nervous system, leading to shorter synaptic neurotransmission latencies and thereby to amelioration of the intellectual impairments.

Another interesting effect of PSL on intellectual ability, demonstrated in the present study, was a significant increase in the IQ scores of patients with nonsense point mutations as compared with those with deletion or duplication mutations (Fig 1D). Premature stop codons caused by nonsense point mutations lead to protein deficiencies and, in many cases, to loss-of-function effects. Read through refers to the treatment effect on patients with specific protein deficiencies resulting from nonsense point mutations. When certain chemical compounds, such as amino glycoside antibiotics, are administered to these patients, they act on ribosomes to read through the premature stop codon, and normal wild-type proteins are thus synthesized, leading to cure of the disease. Because significant increases in IQ scores were observed in patients with nonsense point mutations in this study, we speculated that PSL might exert read-through effects on stop codons and thereby lead to restoration of dystrophin expression in the brain. Our results also raise the possibility that other drugs with read-through effects may improve intelligence in DMD patients.

*Evaluation of motor functions and CK and BNP levels with PSL administration*

Treatment for DMD patients has been attempted with various medication regimens because no definitive therapy exists. At present, PSL is the only medication known to be effective.[28,29] PSL improves muscle strength and motor function as well as delaying the progression of symptoms in DMD patients, although only temporarily. As shown in Fig 2A, the time required to stand up gradually increased in the control group over the course of 2 years. In contrast, the treated group showed no increase in the time required to stand up. We also measured lower limb muscle strength with manual muscle testing because muscle weakness in DMD patients is characterized by reduced proximal muscle strength. Muscle strength was partly maintained in the treated group, while gradual muscle atrophy occurred in the control group (Fig 2B,C).

There are related reports on research that include a previous preliminary study conducted in our laboratory. In that study, PSL was found to increase dystrophin expression in healthy muscles and also in the muscles of DMD patients. An experiment with mdx mice also reportedly demonstrated that PSL administration increased the productions of skeletal muscle dystrophin, spectrin, desmin, and actin proteins.[30]

Although studies have elucidated a relationship between PSL and dystrophin production, more substantial clinical trials are required. In this study, the time required to stand up and lower limb muscle strength both showed improvement and were subsequently maintained in the treated group as compared with the control group. This suggests that PSL administration either stops, or perhaps even partially reverses, the degeneration skeletal muscle.

CK levels did not differ significantly between the treated and control groups (data not shown). Generally, rising CK titers are observed in relation to the amount of muscle contraction and fluctuate based on how much DMD patients move.[31] The mean CK level of 6-year-old male DMD patients without PSL treatment was reported to be 10,611.1 ± 4236.9 IU/L (n = 19). From approximately 10 years of age, CK levels slowly decline but do not recover to normal levels.[32] In the present study, CK levels in patients remained high from the beginning of the treatment period; none of our patients reached normal levels during the follow-up period. Reevaluation under standardized conditions is necessary to examine the relationship between PSL and CK levels.

In this study, although BNP levels were high before PSL administration, BNP had normalized in 73% of patients 1 year after starting PSL treatment (Fig 3). Evaluation at 2 years after starting PSL administration showed that all 15 patients had normal levels. This indicates PSL to be useful for improving BNP levels, again confirming its effectiveness in the treatment of DMD.

## Conclusion

PSL administration significantly ameliorated intellectual impairments in DMD patients, in addition to improving motor function. We observed that patients with nonsense point mutations had more significant increases in IQ scores than those with other gene mutation types such as deletion or duplication, which suggested that PSL might exert a read-through action on stop codons. DMD has been treated with various medications, including PSL, and the results of this study confirm the usefulness of this pharmacologic treatment not only for preserving motor ability, but also for improving intellectual ability in afflicted patients. This is the first study to clinically demonstrate significant intellectual improvement in DMD patients receiving PSL treatment. We anticipate that these results will contribute to future management of DMD patients. Going forward, more detailed investigations are needed. The pharmacologic effects of PSL on cerebral dystrophin as well as the stop codon read-through mechanism require verification in experiments using mdx mice.

We express our deepest gratitude to everyone at the Institute of Medical Genetics of Tokyo Women's Medical University for providing guidance and cooperation. We are also deeply grateful to Mr. Tomoki Uchiyama for statistical analysis. We express our sincere thanks to Professor Makiko Osawa, Tokyo Women's Medical University, who provided us with patient information, and Professor Hitoshi Kanno of the Institute of Medical Genetics and Department of Transfusion Medicine and Cell Processing at Tokyo Women's Medical University, who critically read this manuscript and gave us useful comments.

This study was supported by Intramural Research Grant (No.23-5) for Neurological and Psychiatric Disorders at the National Center of Neurology and Psychiatry (to K.S.), and grants-in-aid from the Research Committee on spinal muscular atrophy, the Ministry of Health, Labour and Welfare of Japan (to K.S.), and by the "Multidisciplinary Education and Research for the Realization of Regenerative Medicine" global Center of Excellence program of the Ministry of Education, Culture, Sports, Science and Technology in 2009.

## References

1. Passamano L, Taglia A, Palladino A, et al. Improvement of survival in Duchenne muscular dystrophy: retrospective analysis of 835 patients. *Acta Myolog.* 2012;31:121-125.
2. Barton-Davis ER, Cordier L, Shoturma DI, Leland SE, Sweeney HL. Amino glycoside antibiotics restore dystrophin function to skeletal muscles of mdx mice. *Clin Invest.* 1999;104:375-381.
3. Dunant P, Walter MC, Karpati G, Lochmüller H. Gentamicin fails to increase dystrophin expression in dystrophin-deficient muscle. *Muscle Nerve.* 2003;27:624-627.
4. Welch EM, Barton ER, Zhuo J. PTC124 targets genetic disorders caused by nonsense mutation. *Nature.* 2007;447:87-91.
5. Dallérac G, Perronnet C, Chagneau C, et al. Rescue of a dystrophin-like protein by exon skipping normalizes synaptic plasticity in the hippocampus of the mdx mouse. *Neurobiol Dis.* 2011;43:635-641.
6. Moxley 3rd RT, Pandya S, Ciafaloni E, Fox DJ, Campbell K. Practice parameter: corticosteroid treatment of Duchenne dystrophy. *Neurology.* 2005;64:13-20.
7. Yamamoto T, Kawano S, Sugiyama D, et al. Predicting scores for left ventricular dysfunction in Duchenne muscular dystrophy. *Pediatr Int.* 2012;54:388-392.
8. Sakurai S, Adachi H, Hasegawa A, et al. Brain natriuretic peptide facilitates severity classification of stable chronic heart failure with left ventricular dysfunction. *Heart.* 2003;89:661-662.
9. Escolar DM, Hache LP, Clemens PR, et al. Randomized, blinded trial of weekend vs daily prednisone in Duchenne muscular dystrophy. *Neurology.* 2011;77:444-451.
10. Bushby K, Muntoni F, Urtizberea A, Hughes R, Griggs R. Treatment of Duchenne muscular dystrophy; defining the gold standards of management in the use of corticosteroids. *Neuromusc Disord.* 2004;14:526-534.
11. Wong BL, Christopher C. Corticosteroids in Duchenne muscular dystrophy: a reappraisal. *J Child Neurol.* 2002;17:183-190.
12. Tsumori M, Inage A. Diagnosis of Mental Development in Infants *[in Japanese]*. Tokyo: Dainippon Tosho; 2005.
13. Mochizuki H, Miyatake S, Suzuki M, et al. Mental retardation and lifetime events of Duchenne muscular dystrophy in Japan. *Intern Med.* 2008;47:1207-1210.

14. Srour M, Bejjani BA, Rorem EA, Hall N, Shaffer LG, Shevell MI. An instructive case of an 8-year-old-boy with intellectual disability. *Pediatr Neurol.* 2008;9:154-155.
15. Cotton SM, Voudouris NJ, Greenwood KM. Association between intellectual functioning and age in children and young adults with Duchenne muscular dystrophy. *Dev Med Child Neurol.* 2005;47: 257-265.
16. D'Angelo MG, Lorusso ML, Civati F, et al. Neurocognitive profiles in Duchenne muscular dystrophy and gene mutation site. *Pediatr Neurol.* 2011;45:292-299.
17. Rao S. Do steroids prolong ambulation and improve quality of life in children with Duchenne muscular dystrophy? *Arch Dis Child.* 2012; 97:1000-1002.
18. Karagan NJ. Intellectual functioning in Duchenne muscular dystrophy. A review. *Psychol Bull.* 1979;86:250-259.
19. Nardes F, Araujo APQC, Ribeiro MG. Mental retardation in Duchenne muscular dystrophy. *J Pediatr.* 2012;88:6-16.
20. Hinton VJ, Fee RJ, Goldstein EM, De Vivo DC. Verbal and memory skill in males with Duchenne muscular dystrophy. *Dev Med Child Neurol.* 2007;49:123-128.
21. Leibowitz D, Dubowitz V. Intellect and Behavior in Duchenne muscular dystrophy. *Dev Med Child Neurol.* 1981;23:577-590.
22. Whitaker S. The stability of IQ in people with low intellectual ability: an analysis of the literature. *Intellect Dev Disabil.* 2008;46:120-128.
23. Mehler MF. Brain dystrophin neurogenetics and mental retardation. *Brain Res Rev.* 2000;32:277-307.
24. Anderson JL, Head SI, Rae C, et al. Brain function in Duchenne muscular dystrophy. *Brain.* 2002;125:4-13.
25. Tracey I, Scott RB, Thompson CH, et al. Brain abnormalities in Duchenne muscular dystrophy: phosphorus-31 magnetic resonance spectroscopy and neuropsychological study. *Lancet.* 1995;345: 1260-1264.
26. Tozawa T, Itoh K, Yaoi T, et al. The shortest isoform of dystrophin (Dp40) interacts with a group of presynaptic proteins to form a presumptive novel complex in the mouse brain. *Mol Neurobiol.* 2012;45:287-297.
27. den Dunnen JT, Casula L, Makover A, et al. Mapping of dystrophin brain promoter: a deletion of this region is compatible with normal intellect. *Neuro Musc Disord.* 1991;1:327-331.
28. Grentzmann G, Inggram JA, Kelly PJ, et al. A dual-luciferase reporter system for studying recoding signals. *RNA.* 1998;4: 479-486.
29. Brooke MH, Fenichel GM, Grigg RC, et al. Clinical investigation of Duchenne muscular dystrophy. Interesting results in a trial of prednisone. *Arch Neurol.* 1987;44:812-817.
30. DeSilva S, Drachman DB, Mellits D, et al. Prednisone treatment in Duchenne muscular dystrophy. *Arch Neurol.* 1987;44:818-822.
31. Skkar RM, Brown Jr RH. Methyl prednisolone increases dystrophin levels by inhibiting myotube death during myogene sis of normal human muscle in vitro. *J Neurol Sci.* 1991;101:73-81.
32. Gilboa N, Swanson RJ. Serum creatine phosphokinase in normal newborns. *Arch Dis Child.* 1976;51:83-85.

Cellular Signalling 26 (2014) 2446–2459

Contents lists available at ScienceDirect

Cellular Signalling

journal homepage: www.elsevier.com/locate/cellsig

# Heterozygous mutations in cyclic AMP phosphodiesterase-4D (PDE4D) and protein kinase A (PKA) provide new insights into the molecular pathology of acrodysostosis

Tadashi Kaname [a,1], Chang-Seok Ki [b,1], Norio Niikawa [c], George S. Baillie [d], Jonathan P. Day [e], Ken-ichi Yamamura [f], Tohru Ohta [g], Gen Nishimura [h], Nobuo Mastuura [i], Ok-Hwa Kim [j], Young Bae Sohn [k], Hyun Woo Kim [l], Sung Yoon Cho [m], Ah-Ra Ko [n], Jin Young Lee [n], Hyun Wook Kim [o], Sung Ho Ryu [o,p], Hwanseok Rhee [q], Kap-Seok Yang [q], Keehyoung Joo [r,s], Jooyoung Lee [r,s,t], Chi Hwa Kim [u], Kwang-Hyun Cho [v], Dongsan Kim [v], Kumiko Yanagi [a], Kenji Naritomi [a], Ko-ichiro Yoshiura [w], Tatsuro Kondoh [x], Eiji Nii [y], Hidefumi Tonoki [z], Miles D. Houslay [aa], Dong-Kyu Jin [m,*]

[a] Department of Medical Genetics, University of the Ryukyus Graduate School of Medicine, Okinawa, Japan
[b] Department of Laboratory Medicine and Genetics, Sungkyunkwan University School of Medicine, Seoul, Republic of Korea
[c] Health Sciences University of Hokkaido, Hokkaido, Japan
[d] Institute of Cardiovascular and Medical Sciences, College of Medical, Veterinary and Life Sciences, University of Glasgow, UK
[e] Department of Genetics, University of Cambridge, Cambridge, UK
[f] Division of Developmental Genetics, Institute of Resource Development and Analysis, Kumamoto University, Kumamoto, Japan
[g] Research Institute of Personalized Health Sciences, Health Sciences University of Hokkaido, Hokkaido, Japan
[h] Department of Pediatric Imaging, Tokyo Metropolitan Children's Medical Center, Tokyo, Japan
[i] Seitoku University, Chiba, Japan
[j] Department of Radiology, Gachon University Gil Medical Center, Incheon, Republic of Korea
[k] Department of Medical Genetics Ajou University Hospital, Ajou University School of Medicine, Suwon, Republic of Korea
[l] Department of Orthopedic Surgery, Yonsei University College of Medicine, Seoul, Republic of Korea
[m] Department of Pediatrics Samsung Medical Center, Sungkyunkwan University School of Medicine, Seoul, Republic of Korea
[n] Clinical Research Center, Samsung Biomedical Research Institute, Seoul, Republic of Korea
[o] Department of Life Sciences, Pohang University of Science and Technology, Pohang, Republic of Korea
[p] Division of Integrative Biosciences and Biotechnology and School of Interdisciplinary Bioscience and Bioengineering, Pohang University of Science and Technology, Pohang, Republic of Korea
[q] Macrogen Inc., Seoul, Republic of Korea
[r] Center for In Silico Protein Science, Korea Institute for Advanced Study, Republic of Korea
[s] Center for Advanced Computation, Korea Institute for Advanced Study, Republic of Korea
[t] School of Computational Sciences, Korea Institute for Advanced Study, Republic of Korea
[u] Mogam Biotechnology Research Institute, Yongin, Republic of Korea
[v] Department of Bio and Brain Engineering, Korea Advanced Institute of Science and Technology (KAIST), Republic of Korea
[w] Department of Human Genetics, Nagasaki University Graduate School of Biomedical Sciences, Nagasaki, Japan
[x] Division of Developmental Disabilities, The Misakaenosono Mutsumi Developmental, Medical and Welfare Center, Isahaya, Japan
[y] Department of Orthopaedic Surgery, Mie Prefectural Kusanomi Rehabilitation Center, Tsu, Japan
[z] Section of Clinical Genetics, Department of Pediatrics, Tenshi Hospital, Sapporo, Japan
[aa] Institute of Pharmaceutical Science, King's College, London, UK

ARTICLE INFO

*Article history:*
Received 14 June 2014
Received in revised form 16 July 2014
Accepted 16 July 2014
Available online 24 July 2014

*Keywords:*
Acrodysostosis

ABSTRACT

Acrodysostosis without hormone resistance is a rare skeletal disorder characterized by brachydactyly, nasal hypoplasia, mental retardation and occasionally developmental delay. Recently, loss-of-function mutations in the gene encoding cAMP-hydrolyzing phosphodiesterase-4D (*PDE4D*) have been reported to cause this rare condition but the pathomechanism has not been fully elucidated. To understand the pathogenetic mechanism of *PDE4D* mutations, we conducted 3D modeling studies to predict changes in the binding efficacy of cAMP to the catalytic pocket in PDE4D mutants. Our results indicated diminished enzyme activity in the two mutants we analyzed (Gly673Asp and Ile678Thr; based on PDE4D4 residue numbering). Ectopic expression of PDE4D mutants in HEK293 cells demonstrated this reduction in activity, which was identified by increased cAMP levels. However,

* Corresponding author at: Department of Pediatrics, Samsung Medical Center, Sungkyunkwan University School of Medicine, Samsung Medical Center, 50 Irwon-dong, Gangnam-gu, Seoul 135-710, Republic of Korea. Tel.: +82 2 3410 3525; fax: +82 2 3410 0043.
*E-mail address:* jindk@skku.edu (D.-K. Jin).
[1] The first two authors (T.K. and C.-S.K.) contributed equally to this work.

http://dx.doi.org/10.1016/j.cellsig.2014.07.025
0898-6568/

PDE4D
cAMP
Knok out rat

the cells from an acrodysostosis patient showed low cAMP accumulation, which resulted in a decrease in the phosphorylated cAMP Response Element-Binding Protein (pCREB)/CREB ratio. The reason for this discrepancy was due to a compensatory increase in expression levels of PDE4A and PDE4B isoforms, which accounted for the paradoxical decrease in cAMP levels in the patient cells expressing mutant isoforms with a lowered PDE4D activity. Skeletal radiographs of 10-week-old knockout (KO) rats showed that the distal part of the forelimb was shorter than in wild-type (WT) rats and that all the metacarpals and phalanges were also shorter in KO, as the name acrodysostosis implies. Like the G-protein α-stimulatory subunit and PRKAR1A, PDE4D critically regulates the cAMP signal transduction pathway and influences bone formation in a way that activity-compromising *PDE4D* mutations can result in skeletal dysplasia. We propose that specific inhibitory PDE4D mutations can lead to the molecular pathology of acrodysostosis without hormone resistance but that the pathological phenotype may well be dependent on an over-compensatory induction of other PDE4 isoforms that can be expected to be targeted to different signaling complexes and exert distinct effects on compartmentalized cAMP signaling.


## 1. Introduction

Acrodysostosis is a group of rare skeletal disorders characterized by brachydactyly, nasal hypoplasia, mental retardation, and occasionally developmental delay [1]. Progressive growth failure, short stature, and severe mid-face hypoplasia with skull deformity are common features of this disorder [1,2]. Acrodysostosis is phenotypically heterogeneous, and at least two groups are recognized: acrodysostosis with hormone resistance (OMIM #101800) and without hormone resistance (OMIM #614613). Acrodysostosis has attracted attention because the disorder shares common skeletal changes with Albright's hereditary osteodystrophy (AHO) or pseudohypoparathyroidism type 1a (PHP-1a). However, neither the biochemical impairment of the activity of G-protein α-stimulatory subunit (GNAS), which activates adenylyl cyclase and cAMP production [3], nor the genetic mutation of GNAS associated with PHP-1a, have been observed in individuals with acrodysostosis [1,4]. Recently, 3 patients with acrodysostosis with hormone resistance were identified to harbor the same nonsense mutation in the *PRKAR1A* gene [5]. The *PRKAR1A* gene encodes the cAMP-binding regulatory subunit of protein kinase A (PKA) that, together with an exchange protein activated by cAMP (Epac) [6], functions as a key intracellular signal transducer in Gsα-cAMP signaling.

Cyclic AMP levels are dynamically regulated not only by the activation of adenylyl cyclase but also by the inhibition of cAMP phosphodiesterases (PDEs), which provide the sole route for inactivation of this second messenger in the cells [7,8]. Of the PDE superfamily, selective inhibitors of the cAMP-specific phosphodiesterase-4 (PDE4) family have been shown to have profound anti-inflammatory actions [9–11] and have demonstrable therapeutic utility in both COPD (roflumilast) [12–14] and psoriatic arthritis (apremilast) [15,16].

Four genes encode the PDE4 family (PDE4A, PDE4B, PDE4C, PDE4D) with alternative splicing generating >20 isoforms [7,17]. A key functional consequence of this diversity is that various signaling scaffold and other proteins are able to sequester specific PDE4 isoforms [7, 18–20]. This tethering leads to the spatial localization of individual types of PDE4 isoforms which act to underpin compartmentalized cAMP signaling by shaping gradients of cAMP in distinct intracellular locales [7]. This ability confers non-redundant functional roles on specific PDE4 isoforms as uncovered using dominant negative [21–24] and siRNA (small interfering RNA)-mediated knockdown [25] approaches. In this, PDE4A1 provides the paradigm for PDE targeting [26–28], while PDE4D5 provides the paradigm for a particular PDE isoform being able to regulate a specific cellular function through targeting [29].

Individual PDE4 isoforms have distinct, intronic promoters that confer cell-type specific patterns of expression. Although little is known about these it has been shown that sustained changes in cAMP levels can alter expression levels of particular PDE4 isoforms, some of which have CRE loci that allows for their regulation by PKA phosphorylated CREB [30–33].

PDE4 isoforms are sub-categorized into long forms with UCR1 and UCR2 regulatory regions; short forms lacking UCR1 and super short forms lacking UCR1 but with a truncated UCR2 [7,34]. When cAMP levels are elevated in cells, the long PDE4 isoforms play a pivotal and exclusive role in determining both the magnitude and duration of this response through their activation through phosphorylation by cAMP-dependent protein kinase A (PKA) [35–43].

PDE4 long isoforms thus play a key role in underpinning both the cellular desensitization to cAMP as well as determining the compartmentalization of cAMP signaling. As such, changes in their activity, localization, post-translational regulation and the complement of different isoforms expressed in a particular cell are set to have profound physiological consequences [7].

Here, we present data collected using 3 approaches. First, in a mutation study, we identified 7 patients with acrodysostosis without hormonal resistance, linking the disease with the gene for cAMP-specific phosphodiesterase 4D (PDE4D). Second, in functional studies, we analyzed the 3D structure of PDE4D mutants and measured the activity of PDE4D mutants transfected into heterologous cells; we also colocalized PDE4D and β-arrestin using confocal microscopy and determined PDE4 activity and isoform expression in patient cells. Third, we generated PDE4D knockout (KO) rats and demonstrated that PDE4D loss results in the skeletal dysplasia phenotype observed in acrodysostosis. This work opens up a new horizon in the pathogenesis of acrodysostosis by showing that acrodysostosis without hormone resistance can be caused by alterations in cAMP degradation by PDE4D [7] and results in skeletal dysplasia.

## 2. Methods

### 2.1. Patient enrolment

Seven patients diagnosed as acrodysostosis without hormone resistance were included in the study. The patients represent all of the available patients diagnosed at the time of the study in Korea and Japan. Diagnosis was made by the typical X-ray features and the confirmation of the absence of the hormone resistance. The details of clinical features including hormone profiles are described in Table 1. One patient diagnosed as acrodysostosis without hormone resistance, who harbor the *PRKAR1A* mutation was included in the functional study for comparison.

The clinical features of 1 Korean (patient 2) and 3 Japanese patients (patients 4, 5 and 7) were described previously [44–46]. The mother of the Japanese siblings (patients 4 and 5) was reported to be affected mildly. For the other patients, clinical features are summarized in Table 1. Informed consent was obtained from the parents of all patients and this study was approved by the Institutional Review Board.

### 2.2. DNA study

Exome sequencing was performed on 2 Korean patients and 2 Japanese siblings with acrodysostosis (4 patients in 3 families), as well

**Table 1**
Clinical and laboratory findings of patients
Identifying mutations in acrodysostosis patients. Exomes were sequenced in 8 patients with acrodysostosis. We found that patient 8 had a de novo p.Arg368* mutation in *PRKAR1A*. When we compared the gene lists from patients other than patient 8, *PDE4D* was identified as the only gene they all shared.

| | Patient 1 | Patient 2 | Patient 3 | Patient 4 | Patient 5 | Patient 6 | Patient 7 | Patient 8 | Reference range |
|---|---|---|---|---|---|---|---|---|---|
| Previous reports | Unpublished | Ref 9 | Unpublished | Ref 8 | Ref 8 | Unpublished | Ref 10 | Unpublished | |
| Gene | *PDE4D* | *PDE4D* | *PDE4D* | *PDE4D* | *PDE4D* | *PDE4D* | *PDE4D* | *PRKAR1A* | |
| Mutation | c.2033 T > C (p.I678T) | c.2018G > A (p.G673D) | c.2033 T > C (p.I678T) | c.683A > C (p.Q228P) | c.683A > C (p.Q228P) | c.689 T > C (p.L230S) | c.1759A > G (p.T587A) | c.1101C > T (p.R368X) | |
| *Clinical findings* | | | | | | | | | |
| GA (wk)/ Bwt (kg) | 40/2.8 | 40/2.9 | 41/2.3 | 40/2.22 | 40/2.35 | 41/2.5 | 38/2.3 | 37 + 4/2.08 | |
| Sex/age (y) | F/17 y | M/17 y | M/4 y 11 m | F/39 y | M/37 y | M/10 y 5m | F/8 y 5 m | M/3 y 9 m | |
| Height (cm)/ SD | 144.7/−3.1 | 155/−2.8 | 98.8/−1.4 | 149/-2.1 | 135/-5.9 | 137.2/-0.9 | 131.6/-0.2 | 95.6/−1.7 | |
| Weight (kg)/ SD | 54/−0.1 | 57/−0.7 | 15/-1.6 | 54.3/0 | 42.3/-2.2 | 37.2/-0.6 | 31/0.2 | 15.7/−0.6 | |
| Short nose with flat nasal bridge | + (Nose vestigial) | + (Nose vestigial) | + | + (Nose vestigial) | + (Nose vestigial) | + (Nose vestigial) | + (Nose vestigial) | + | |
| Prominent forehead | + | + | + | + | + | + | + | + | |
| Iris color at infancy* | Light brown | Black | Gray | Gray | Gray | Gray | Gray > brown | Gray | |
| Mental retardation | Mild | Severe | Severe | Severe | Severe | Mild to Severe | Severe | Mild | |
| Developmental milestone | Delayed | Delayed | Delayed | Delayed | Delayed | Delayed | Delayed | Normal | |
| *Radiologic findings* | | | | | | | | | |
| Peripheral skeletal dysplasia | Severe | Severe | Severe | Severe | Severe | Severe | Severe | Mild | |
| Nasomaxillary hypoplasia | Severe | Severe | Severe | Severe | Severe | Severe | Severe | Mild | |
| Brachydactyly | Severe | Severe | Severe | Severe | Severe | Severe | Severe | Mild | |
| Advanced bone age | Yes | Yes | Yes | Yes | Yes | Yes | Yes | Yes | |
| *Laboratory findings* | | | | | | | | | |
| Hormonal resistance | No | No | No | No | No | No | No | Yes | |
| PTH/Ca/P | 34/9.8/3 | 9/4.1 | NA/10.2/4.5 | 64.4/9.4/3.2 | 61.7/9.3/3.4 | 41/9.6/4.4 | NA/9.8/5.3 | 56/9.5/5.0 | PTH: 11–62 pg/ml<br>Ca: 8.4–10.2 mg/dl<br>P: 2.5–4.5 mg/dl |
| 25-vit. D | 15.29 | NA | NA | NA | NA | NA | NA | 34.52 | 8–51.9 mg/dl |
| fT4/TSH | 1.54/2.25 | 1.17/0.91 | 1.5/1.54 | 1.25/1.25 | 1.26/0.41 | 1.6/1.79 | 1.15/NA | 0.98/67.51 | fT4: 0.89–1.8 ng/dl<br>TSH: 0.35–5.5 uIU/ml |
| hGH | 0.05 | NA | NA | NA | NA | NA | NA | 0.82 | 0–4.7 ng/ml |
| IGF-1 | 210.8 | 272.3 | 112.6 | NA | NA | NA | NA | 152.6 | 49–642 ng/ml |
| LH/FSH | 3.1/6.3 | 5.5/3.5 | NA | NA | NA | NA | 0.1>/1.8 | 1.2/1.5 | LH: 0–10.6 uIU/ml<br>FSH: 0.1–9 uIU/ml |
| ACTH | 9.9 | NA | NA | NA | NA | NA | 88.3 | 34.8 | 0–60 pg/ml |
| Estradiol | 39 | 2.95 | NA | NA | NA | 0.11 | NA | <0.01 | Estradiol: 10–441 pg/ml |
| Testosterone** | | | | | | | | | Testosterone: 2.79–8.76 ng/ml |

* Reference cDNA sequence: NM_001104631.

as on the family members of the Korean patients (both parents and a brother of patient 1; mother and a sister of patient 2; and both parents of patient 8). After identifying the causative gene, exomes of 3 unrelated Japanese patients were also analyzed.

*2.2.1. Exome sequencing*

*2.2.1.1. Library construction.* Each sample that was sequenced was prepared according to Illumina protocols. Briefly, 1 μg of genomic DNA was fragmented by nebulization, the fragmented DNA was repaired, an 'A' was ligated to the 3′ end of fragments, Illumina adapters were then ligated to the fragments, and the samples were size selected, aiming for products of 350–400 base pairs. The size-selected products were amplified using PCR, and each final product was validated using Agilent Bioanalyzer. Before first hybridization, multiple libraries with distinct indices were combined into a single pool and then enrichment. The pooled DNA libraries were mixed with the "capture" probes against the targeted regions and incubated for the recommended hybridization time, which ensured that the targeted regions bound completely to the capture probes. Streptavidin beads were used to capture the probes bound to the targeted regions and the beads were washed thrice to remove non-specifically bound DNA. The enriched library was then eluted from the beads and prepared for a second hybridization. The DNA library obtained from the first elution was mixed with the capture probes against the target regions, and the second hybridization ensured that the targeted regions were enriched further. Streptavidin beads were used again to capture the probes containing the targeted regions and the beads were washed thrice to eliminate non-specifically bound DNA. The library thus enriched was eluted from the beads and prepared for sequencing. PCR was used to amplify the enriched DNA library for sequencing. PCR was performed using the same PCR primer cocktail used in TruSeq DNA Sample Preparation. Axeq Technologies conducted quality-control analysis on the sample library and quantified the DNA library templates.

*2.2.1.2. Clustering and sequencing.* Illumina used a unique "bridged" amplification reaction that occurs on the surface of the flow cell. A flow cell containing millions of unique clusters was loaded into HiSeq 2000 for automated cycles of extension and imaging.

*2.2.1.3. Extension and imaging.* Solexa's Sequencing-by-Synthesis used 4 proprietary nucleotides possessing reversible fluorophore and termination properties. Each sequencing cycle occurred in the presence of all 4 nucleotides, leading to a higher accuracy than with methods where a single nucleotide at a time is present in the reaction mix. This cycle was repeated, one base at a time, generating a series of images, each representing a single base extension at a specific cluster.

*2.2.1.4. Sequence analysis.* Paired-end sequences produced by HiSeq 2000 were mapped to the human genome, where the reference sequence was the UCSC assembly hg19 (NCBI build 37), without unordered sequences and alternate haplotypes; the mapping program used was BWA (version 0.5.9rc1). Uniquely mapped reads were only included for the latter steps. After generating a consensus sequence by creating a pileup file from the BAM file, a variant-calling process was run using SAM tools (version 0.1.12a), at which stage candidate SNPs and short indels were detected at nucleotide resolution. These variants were then annotated using ANNOVAR (version 2011Jun18) based on functional predictions, including SIFT and PolyPhen, to filter SNPs from the dbSNP for versions of 131 and 132, and to search SNPs from the 1000 Genomes project. Finally, in-house scripts and open programs were used to estimate various numbers obtained from all stages.

For consistency, the PDE4D residue numbering that we adopt here is based on the reference PDE4D4 isoform (GenBank accession No. NP_001098101) because the Leiden Open Variation Database (LOVD) of human Mendelian genetic variation uses human PDE4D4 (NP_001098101) as the reference sequence.

*2.2.2. Sanger sequencing*

Genomic DNA was extracted from peripheral blood leukocytes using Wizard Genomic DNA Purification kit, following the manufacturer's instructions (Promega). *PDE4D* exons and their flanking introns were amplified using primer sets we designed (available upon request). PCR was performed using a thermal cycler (model 9700, Applied Biosystems) as follows: 32 cycles of denaturation at 94 °C for 30 s, annealing at 60 °C for 30 s, and extension at 72 °C for 30 s. After treating the amplicon (5 μL) with 10 U of shrimp alkaline phosphatase and 2 U of exonuclease I (USB Corporation), direct sequencing was performed using a BigDye Terminator Cycle Sequencing Ready Reaction kit (Applied Biosystems) on an ABI Prism 3130xl genetic analyzer (Applied Biosystems). Novel *PDE4D* variants were confirmed on more than 2000 ethnicity-matched control chromosomes by sequencing. To describe sequence variations, we followed the guidelines of the Human Genome Nomenclature Committee (HGVS); the 'A' of the ATG translation start site was numbered +1 in DNA sequences and the first methionine was numbered +1 in protein sequences.

*2.3. Functional studies*

The disease-associated mutants are denoted as per PDE4D4 as the LOVD of human Mendelian genetic variation using human PDE4D4 (NP_001098101) as the reference sequence. This particular isoform is not widely expressed and is found predominantly in the brain [47]. We, have thus made and functionally characterized these mutations in the commonly expressed PDE4D5 isoform [47].

To predict the structural change in PDE4D mutations, molecular modeling and docking simulation of wild-type (WT) and mutant PDE4D were conducted, and we tested whether overexpression of recombinant WT or mutant PDE4D5 proteins affects the intracellular cAMP levels in HEK293 cells after treating with the adenylyl cyclase activator, forskolin.

Next, we measured the cAMP-hydrolyzing activity of the PDE4D mutant in Epstein–Barr virus (EBV)-transformed lymphocytes from patient 8 (with *PRKAR1A* p.R368* mutation) and patient 6 (with *PDE4D* p.L230S mutation), and we determined the phosphorylated Cyclic AMP Response Element-Binding Protein (pCREB):CREB ratio in the patient cells by Western blotting. We also measured total PDE and PDE4-specific activity to determine whether *PDE4D* mutations affect cAMP hydrolysis in the EBV-immortalized lymphocytes from the patients and control subjects. We determined the total cAMP-hydrolyzing activity in the presence or absence of the pan-PDE inhibitor IBMX, which inhibits all cAMP-hydrolyzing PDEs except PDE8 [8]. We also conducted these assays in the presence of the PDE4-specific inhibitor rolipram [8–11] to estimate the PDE4 fraction of total PDE activity. Lastly, we measured the expression of PDE4 and its isoforms in the patient cells and control cells.

*2.3.1. Molecular modeling and docking simulation of wild-type and mutated PDE4D*

We built 3D structural models for the catalytic domain of the PDE4D wild-type (WT) and its 2 mutants (p.Gly673Asp and p.Ile678Thr; based on PDE4D4). In PDB, several X-ray structures of PDE4D are available, and their overall structures are similar to each other and display a conserved shape for the cAMP-binding pocket. For 3D modeling, we employed a recently proposed high-accuracy template-based modeling method [48]. This method based on global optimization was shown to be successful in recent CASP7 and CASP8 protein-structure prediction experiments [49–51]. A total of 9 templates were used as core templates (3G4G, 1ZKN, 1OYN, 1ROR, 3LY2, 3G4I, 2QYK, 3DYN, and 2OUR), and 4 additional templates were used in a combinatorial manner (2H44, 1TBF, 3JWQ, and 3ITU) to consider 16 possible template combinations. The

final 3D model of each target sequence was selected from among 1600 candidate models by assessing their quality and comparing their structure with the X-ray structure of WT PDE4D (3G4I). The final models were all similar to 3G4I, with backbone RMSDs being approximately 0.4 Å ($0.4 \times 10^{-10}$ m). To estimate the binding affinity between the protein 3D models and cAMP, we performed docking simulations by using AutoDock Vina [52], a new and improved version of AutoDock. We performed flexible docking by considering these 14 flexible side-chains around the cAMP-binding pocket of PDE4D4: D503, D620, Q671, N623, G673 (D673 for p.Gly673Asp), I678 (T678 for p.Ile678Thr), Y461, H462, H466, H502, M575, L621, I638, and F642. A total of 30 exhaustive docking simulations were performed for each protein model.

*2.3.2. CREB phosphorylation assay*

For Western blotting analysis of phosphorylated-CREB levels in cells, EBV-transformed lymphocytes or HEK293 cells were harvested, washed with phosphate buffered saline (PBS), and lysed in RIPA buffer. Proteins were quantified using the BCA assay (Pierce). Equal amounts of whole cell lysates were separated using SDS-polyacrylamide gel electrophoresis (SDS-PAGE) and transferred to nitrocellulose membranes. Western blotting was performed using antibodies against CREB phosphorylated at Ser133 (pCREB) and total CREB (Cell Signaling Technology). Blots were developed using a peroxidase-conjugated secondary antibody and ECL Plus Western Blotting Detection System (Amersham™).

*2.3.3. Quantification of cAMP*

The cAMP-measuring kit was purchased from R&D Systems (Abingdon); cellular cAMP concentrations were measured using the competitive-binding technique, according to the manufacturer's instructions.

*2.4. Generation of PDE4D knockout rats*

The PDE4D knockout (KO) rats were generated and provided by Transposagen Biopharmaceuticals (Lexington, KY). Pde4d$^{Tn(sb\text{-}T2/Bart3)2.285Mcwi}$ on an F344 background was produced by a single-gene trap method based on the Sleeping Beauty transposable element [53]. After confirming trap-vector insertion in the 1st intron of *PDE4D*, rats homozygous for the PDE4D-targeted KO mutation were mated and pups were used for further analyses.

## 3. Results

*3.1. Patient profiles and mutations*

Seven patients diagnosed as acrodysostosis without hormone resistance were included in the study. The clinical and molecular characteristics of the patients are summarized in Table 1, and detailed mutation profiles and radiographs of patients are presented in Fig. 1A–J. The disease-associated mutants are denoted as per PDE4D4 as the LOVD of human Mendelian genetic variation uses human PDE4D4 (NP_001098101) as the reference sequence [47].

*3.2. Three dimensional structure analysis of PDE4D mutants*

Analyzing the 3D structure of the PDE4D mutants predicted changes in the binding efficacy of cAMP to the catalytic pocket in PDE4D mutants, indicating diminished enzymatic activity in the mutants (Table 2 and Fig. 2).

Cartoon figures of protein backbone structures (WT, p.Gly673Asp, and p.Ile678Thr; based on PDE4D4) with bound cAMP are shown in superposition in Fig. 2. The 3D models show few structural differences between WT and the 2 mutants in their backbones and side-chains, except for the mutated residues. The 2 mutated residues (p.Gly673Asp and p.Ile678Thr), which are positioned at the right-hand side of the cAMP-binding pocket, are represented by purple stick figures in Fig. 2B. Table 2 shows the average lowest binding affinity in a docking simulation between PDE4D and its substrate, cAMP. We observed that the WT protein was slightly more stable with cAMP, by approximately 0.17 kcal/mol, than the 2 mutants. This is because the WT and mutants have the same conserved binding residues (D503, D620, and Q671) around the cAMP-binding site, according to the Uniprot annotation; consequently, the binding conformations that correspond to the lowest binding energy are nearly identical, with only small variations in side-chain conformation around cAMP (Fig. 2B). The lowest binding energy and the number of successful bindings of each protein model are shown in Table 2. A successful binding corresponds to the formation of appropriate hydrogen bonds between cAMP and the binding residues of each protein (Fig. 2B). The standard deviation was calculated from 30 independent docking simulations. For WT PDE4D, all 30 simulations resulted in the same successful docking conformation that is shown in Fig. 2B. By contrast, the lowest energy binding conformations of the 2 mutants were found only 4 and 9 times out of 30 simulations (Fig. 2B), implying that the mutated residues entropically deter the binding of cAMP to the catalytic pocket and possibly affect enzymatic activity. The multiple sequence alignment used for 3D modeling showed that G673 is conserved and I678 is either conserved or substituted by a similar hydrophobic residue such as Val.

The Gly673Asp mutation results in the small neutral Gly residue in the WT protein being exchanged for a bulky negatively charged Asp residue. This Asp residue in the mutant could potentially interact with the –OH of cAMP and either block or inhibit cAMP entry into the binding pocket, thereby preventing efficient catalysis.

The Ile678Thr mutation exchanges a hydrophobic Ile residue for a hydrophilic Thr residue. Hydrophobic residues generally shield hydrogen bonds that form between the ligand and the protein in the catalytic pocket by providing a protective hydrophobic cap. Therefore, ablation of this hydrophobicity by the replacement with hydrophilic Thr likely interferes with critical internal hydrogen bonds between the protein and cAMP, and could therefore attenuate effective catalysis.

*3.3. Functional studies on PDE4D mutants*

*PDE4D* encodes a series of isoforms generated through the use of alternative promoters and alternative mRNA splicing. These isoforms are characterized by unique N-terminal regions that are invariably employed to target them to specific signaling complexes in cells, thereby conferring the unique functionality of the PDE4D isoforms [7,19]. The reference PDE4D isoform, PDE4D4 isoform is not widely expressed and is found predominantly in the brain [47]. We, have thus made and functionally characterized these mutations in the commonly expressed PDE4D5 isoform [47].

We assessed the functional activity of the Gsα-cAMP-PKA signal transduction pathway in the cells by measuring cAMP hydrolysis and the phosphorylation status of CREB, which is a pivotal target for PKA action. PDE4D5 is a common PDE4D long isoform responsible for desensitizing cAMP signals that arise from Gs-coupled cell-surface receptors [54]. We analyzed whether overexpressing recombinant WT or mutant PDE4D5 proteins affects intracellular cAMP levels in HEK293 cells treated with forskolin, which activates adenylyl cyclase. Whereas overexpressing WT PDE4D5 markedly lowered forskolin-stimulated cAMP levels, overexpressing Q228P-, G673D-, and I678T-PDE4D5 mutants at similar expression levels did not (Fig. 3A).

Next, we measured the cAMP-hydrolyzing activity of PDE4D mutants in EBV-transformed lymphocytes from patient 8 (with *PRKAR1A* p.R368X mutation) and patient 6 (with *PDE4D* p.L230S mutation). The cAMP level in the cells from patient 6 was significantly lower at 30 min after treatment with forskolin when compared to the cells from the control subject ($P = 0.02$, Fig. 3B).

Western blotting demonstrated that the pCREB to CREB ratio was significantly decreased in the cells from both patients 6 and 8 when

compared with the cells from the control subject (Fig. 3C and D): the basal level of pCREB in EBV-transformed cells from both patients was lower than in the control cells (Fig. 3C), and, after a 30-min treatment with forskolin, lower levels of pCREB were detected in the cells from the patients than in control (Fig. 3D). All cells had similar total CREB levels (Fig. 3B and D).

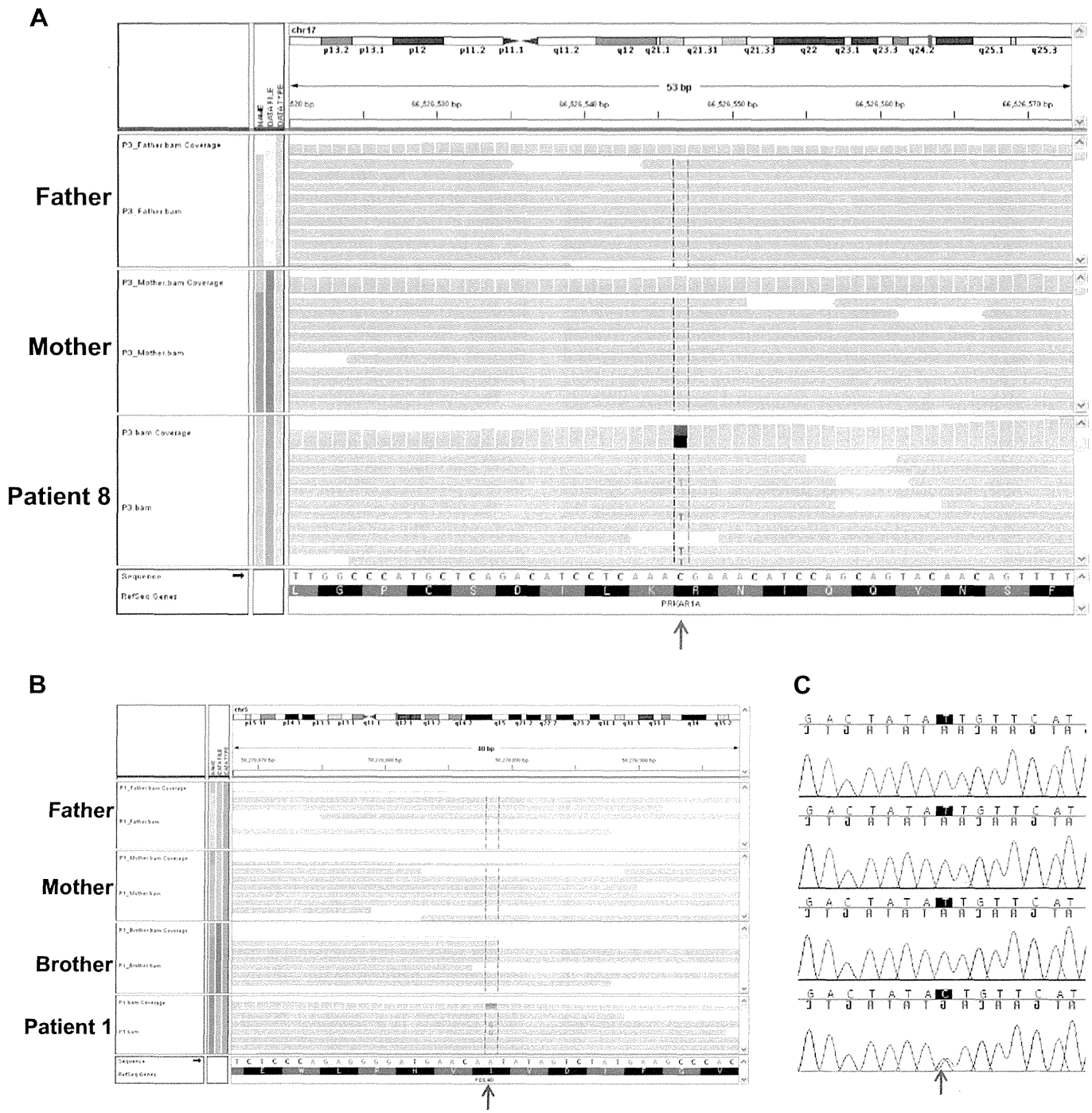


**Fig. 1.** Identification and confirmation of *PRKAR1A* and *PDE4D* mutations. A; The IGV browser view of the *PRKAR1A* gene region from the exome sequencing data shows that patient 8 (bottom panel) has the c.1101C > T (p.Arg368X) mutation in the *PRKAR1A* gene (arrow), but the father (top panel) and mother (middle panel) have the WT sequence. B; The IGV browser view of the *PDE4D* gene region from the exome sequencing data shows that patient 1 (bottom panel) has the c.2033 T > C (p.Ile678Thr) mutation in the *PDE4D* gene (arrow), but the father (top panel), mother (upper middle panel), and brother (lower middle panel) have the WT sequence. C; Sanger sequencing confirmed that patient 1 has a heterozygous mutation (c.2033 T > C; p.Ile678Thr) in the *PDE4D* gene (arrow), whereas the other family members have WT sequences. D; The IGV browser view of the *PED4D* gene region from the exome sequencing data shows that patient 2 (bottom panel) has the c.2018G > A (p.Gly673Asp) mutation in the *PDE4D* gene (arrow), but the mother (top panel) and sister (middle panel) have the WT sequence. E; Sanger sequencing confirmed that patient 2 has a heterozygous mutation (c.2018G > A; p.Gly673Asp) in the *PDE4D* gene (arrow), whereas the other family members have WT sequences. F; A comparison of the protein sequences of human, chimpanzee, orangutan, dog, mouse, and zebra fish orthologs of PDE4D shows that p.Gly673 and p.Ile678 are highly conserved residues. G; The IGV browser view of the *PED4D* gene region from the exome sequencing data shows that patient 4 (upper panel) and patient 5 (lower panel) have the c.683A > C (p.Gln228Pro) mutation in the *PDE4D* gene (arrow). H; Sanger sequencing confirmed that patients 4 and 5 have a heterozygous mutation (c.683A > C; p.Gln228Pro) in the PDE4D gene (arrow). I; Schematic diagram and Sanger sequencing of 3 mutations detected in the *PDE4D* genes in patients 6, 7, and 3. Mutations are indicated on a PDE4D protein structure with conserved domains. P: phosphorylation sites. UCR: upstream conserved region. J; X-ray views of hands and feet of patients 1, 2, and 8 revealing typical characteristics of acrodysostosis: shortening of the metacarpals, metatarsals, phalanges, and cone-shaped epiphyses. Patients 1 and 2 showed more severe bony abnormalities than patient 8.

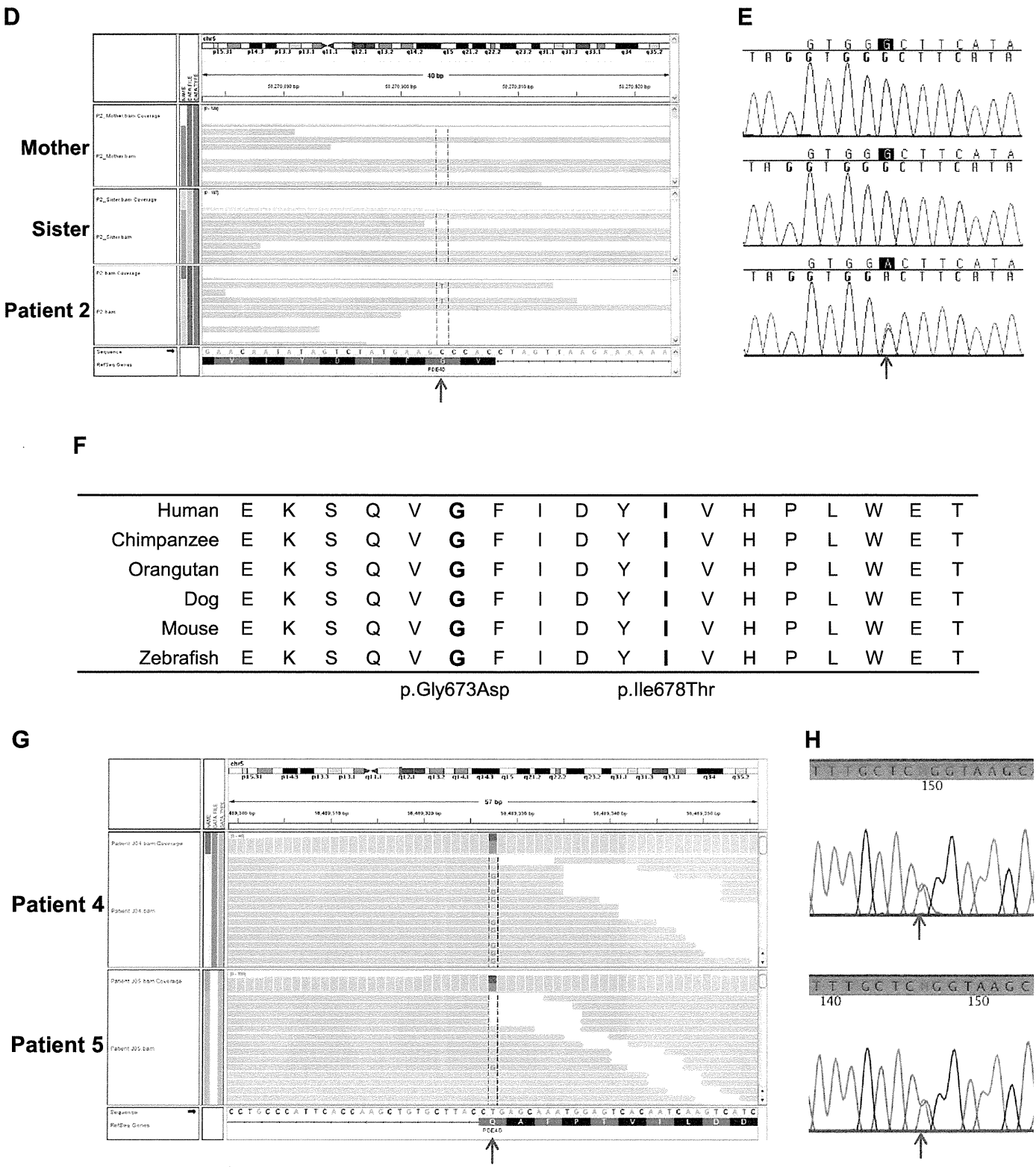


**Fig. 1** (*continued*).

### 3.4. PDE4-specific activity

We investigated the activity of the PDE4 mutants found in patients to determine whether the mutations affect the cAMP-hydrolyzing capability of the enzyme. Five distinct PDE4D mutant constructs (Q164P, L166S, T523A, G609D, and I614T; based on PDE4D5 [47], Table 3) were overexpressed in HEK293 cells and lysates containing equal amounts of WT and mutant PDE4D proteins were used to assess the proteins' ability to hydrolyze cAMP (Fig. 3A). Relative to WT PDE4D, all the PDE4D mutants exhibited markedly diminished cAMP-hydrolyzing activity. Therefore, inserting the PDE4 gene mutations found in patients with acrodysostosis without hormone resistance into PDE4D4 severely compromised the catalytic activity of PDE4D4.

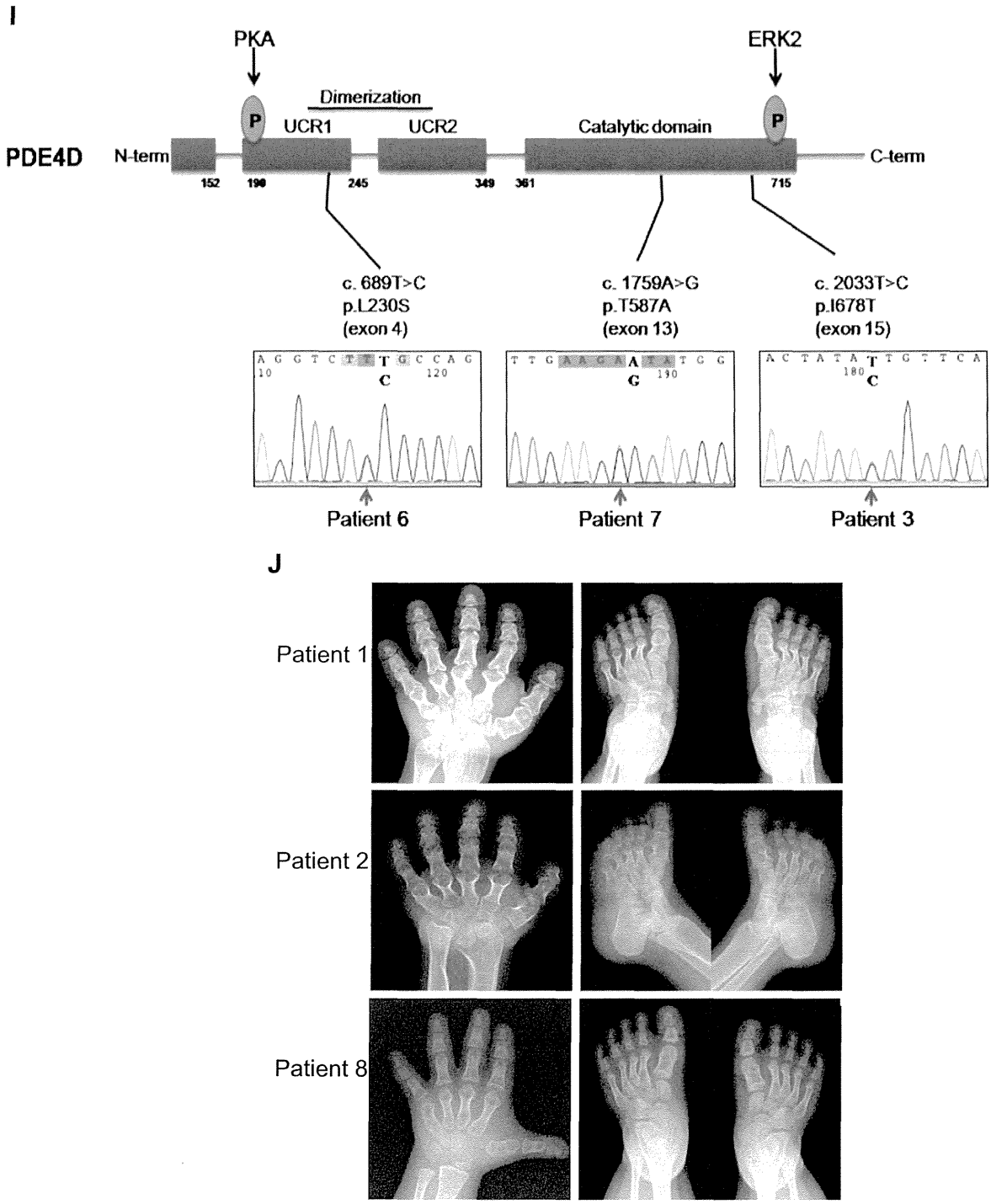


**Fig. 1** (*continued*).

Next, we measured the cAMP PDE activity in EBV-immortalized lymphocytes from control subjects and patients. We determined the total cAMP-hydrolyzing activity in the presence or absence of the pan-PDE inhibitor IBMX, which inhibits all cAMP-hydrolyzing PDEs except PDE8 [8]. We also conducted these assays in the presence of the PDE4-specific inhibitor Rolipram, which enabled us to estimate the fraction of total PDE activity that was due to PDE4 [55]. This allowed us to compare both total PDE and PDE4-specific cAMP-hydrolyzing activity in the control subject and in the PDE4D-mutated patient 6 (Fig. 4). Surprisingly, we found that patient 6 exhibited total PDE and PDE4-specific activities that were similar to those of the control subject. This may be

**Table 2**
The average binding affinities of PDE4D WT and mutants (p.Gly673Asp and p.Ile678Thr). Standard deviations of the binding affinity shown in parenthesis were calculated based on 30 flexible docking simulations. The WT protein is slightly more stable with cAMP (by approximately 0.17 kcal/mol) than the 2 mutants. The number of successful bindings of cAMP to the binding pocket is 30 for WT protein and 4 and 9 for the 2 mutants.

| Models | Average binding affinity (kcal/mol) | Number of successful binding of the 30 trials |
|---|---|---|
| WT | −8.70 (±0.000) | 30 |
| p.Gly673Asp (Pt 2) | −8.51 (±0.311) | 4 |
| p.Ile678Thr (Pt 1) | −8.56 (±0.292) | 9 |

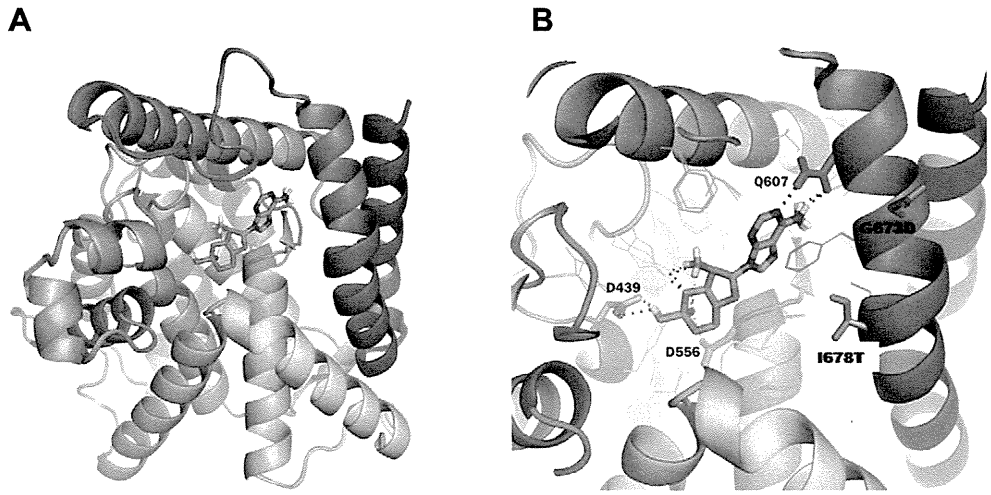


**Fig. 2.** Three dimensional structural models of the catalytic domain of PDE4D. Panel A shows the protein model of WT PDE4D with cAMP and panel B shows the models of the mutants (p.Gly673Asp and p.Ile678Thr) with cAMP. The 3 structures were superposed using the pyMOL program, and the cAMP ligand is positioned at the lowest-energy binding site found in the docking simulation. The binding between the protein and cAMP is shown in detail. D503, D620, and Q671 are known to be conserved binding residues. Side-chains of G673D and I678T are depicted by purple stick figures on the right-hand side of the binding pocket.

because PDE4D isoforms contribute little to the total PDE4 activity in these cells, or because in patient 6 the loss of PDE4D activity was compensated for by the up-regulation of catalytically functional PDE4 from other subfamilies.

### 3.5. Expression of PDE4 and its isoforms in patient cells

We sought to determine if the expression of PDE4 from other subfamilies was altered in patient 6, and we found a dramatic increase in PDE4C expression in the patient (Fig. 4D). By contrast, no changes were detected in the expression of PDE4A and PDE4B subfamilies (Fig. 4D). We also noted that *PDE4D5* and *PDE4D11* mRNA levels in the cells from patient 6 were double than that in control cells (Fig. 4D). This increase in transcripts correlated with an elevated PDE4D5 protein level relative to control, which was shown by staining by a PDE4D5-specific antibody (Fig. 4E).

Our expression-analysis data indicate that in patient 6, the loss of PDE4D activity was compensated for not only through the up-regulation of PDE4D5 and PDE4D11, which would be catalytically compromised, but also through the up-regulation of PDE4C. We propose that these changes help compensate for the reduced catalytic activity of PDE4D isoforms and could explain why total PDE4 activity was almost identical in the EBV-immortalized lymphocytes obtained from the control subject and patient 6 (Fig. 4, A–C).

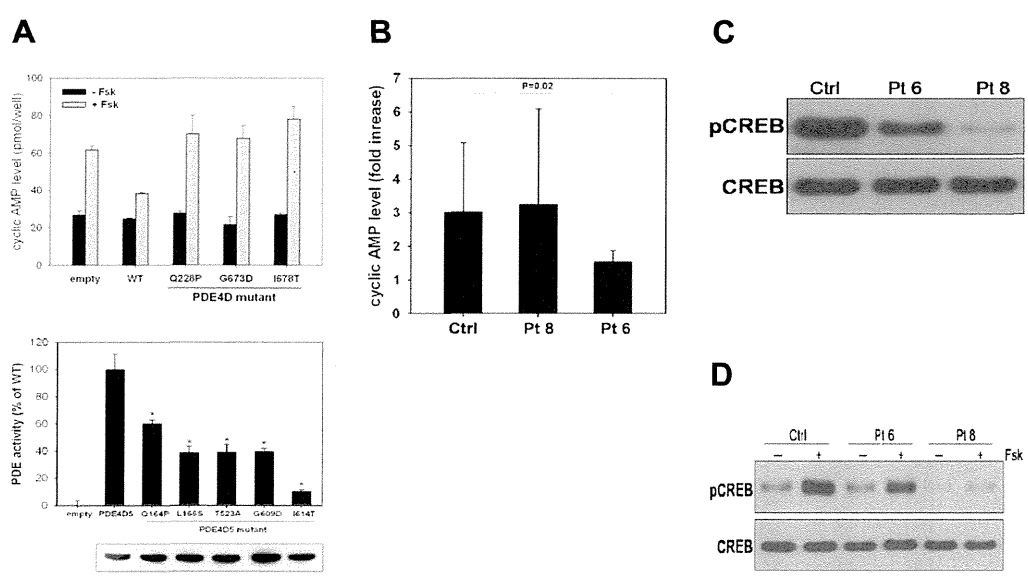


**Fig. 3.** Phosphorylation of cAMP responsive element-binding (CREB) protein in acrodysostosis patients. A. Functional studies on PDE4D in HEK 293 cells. Panel A shows measurement of cAMP in HEK293 cells transfected PDE4D5 WT and mutant constructs. Because the PDE4D isoform is the major species that has cAMP-hydrolyzing activity, we analyzed whether overexpressing recombinant WT or mutant PDE4D affects the cellular level of cAMP in HEK293 cells after treatment with the adenylyl-cyclase activator forskolin (Fsk, 10 μM). WT PDE4D decreased cellular cAMP levels, but overexpressed Q228P-, G673D-, and I678T-PDE4D mutants did not. Panel B shows the total PDE activity of PDE4D constructs. Compared to WT, all of PDE4D mutants had significantly reduced PDE activity. The results are shown as means ± SD. B. Levels of cAMP in EBV-transformed lymphocytes of control subject, patient 8, and patient 6 after treatment with forskolin (Fsk, 10 μM). In cells from patient 6 (with L230S mutation), cAMP levels showed a statistically significant decrease compared to control EBV-transformed lymphocytes. C. Phosphorylated CREB levels in control, patient 6, and patient 8 cells; both patients had lower than control pCREB levels. D. Diminished pCREB levels in patient cells were observed clearly after stimulating with Fsk for 30 min.

**Table 3**
PDE4D isoforms with mutation residue numbers.

| PDE4D4 | D1 | D2 | D3 | D5 | D6 | D7 | D8 | D9 | D10* | D11* |
|---|---|---|---|---|---|---|---|---|---|---|
| Type | Short | Short | Long | Long | Short | Long | Long | Long | Short | Short |
| Q228P | N/A | N/A | 92 | **164** | N/A | 167 | 106 | 98 | N/A | 118 |
| L230S | N/A | N/A | 94 | **166** | N/A | 169 | 108 | 100 | N/A | 120 |
| T587A | 363 | 285 | 451 | **523** | 296 | 526 | 465 | 457 | 283 | 477 |
| G673D | 449 | 371 | 537 | **609** | 382 | 612 | 551 | 543 | 369 | 563 |
| I678T | 454 | 376 | 542 | **614** | 387 | 617 | 556 | 548 | 374 | 568 |

N/A — not applicable as mutation not in N-terminal portion of short form sequence. All clones are human except where indicated*, which are murine clones. The GenBank flat file numbers used are indicated in parentheses PDE4D1 (NP_001184151), PDE4D2, PDE4D3 (NP_006194), PDE4D4 (NP_001098101), PDE4D5 (NP_001184147), PDE4D6 (NP_001184152), PDE4D7 (NP_001159371), PDE4D8 (NP_001184148), PDE4D9 (NP_001184149), PDE4D10 (ABG57277) and PDE4D11 (ACA66114).

### 3.6. Immunofluorescent staining of EBV-transformed B cells

Immunofluorescence staining for PDE4D and the PDE4D scaffold proteins [7,22,56], RACK1 and β-arrestin, demonstrated similar colocalization in patient and control cells of PDE4D (Fig. 5).

### 3.7. PDE4D-KO rats

The role of *PDE4D* mutations in acrodysostosis was clarified by generating a PDE4D-KO rat. Body lengths measured at the ages of 3 and 5 weeks indicated significantly stunted growth in both male and female KO rats relative to WT rats (3 weeks: male to male, $P < 0.001$, female to female, $P < 0.001$; 5 weeks: male to male, $P < 0.001$, female to female, $P = 0.002$, Fig. 6A); stunted growth was observed in the KO and heterozygous rats compared to WT rats at 3 weeks ($P < 0.001$, Fig. 6B).

Skeletal radiographs of 10-week-old KO rats showed that the distal parts of the forelimbs (radius and palm) were shorter than in WT rats, and that all metacarpals and phalanges were shorter in KO rats than in WT rats (Fig. 6C and D).

## 4. Discussion

In this study, we have shown that *PDE4D* mutations are associated with acrodysostosis without apparent hormone resistance. The *PDE4D* gene encodes proteins that critically regulate Gsα-cAMP signaling by modulating the compartmentalization of this key signaling system through targeted cAMP degradation [7,19,57].

PDE4D-family enzymes hydrolyze cAMP and tightly regulate the Gsα-cAMP signal transduction pathway that employs PKA and Epac as its core effectors [7,54]. The *PDE4D* gene is associated with several distinct diseases or traits including ischemic stroke, neuroticism, asthma, and esophageal cancer [58–61]. Our work and 2 recently reported studies [62,63] implicate *PDE4D* as a third gene associated with Gsα-cAMP signaling-linked disorders; the others are *GNAS*, whose mutations are implicated in PHP-1a, pseudo-pseudohypoparathyroidism (PPHP), and progressive osseous heteroplasia (POH), and whose methylation defect is implicated in PHP-1b, and *PRKAR1A*, a nonsense mutation which is associated with acrodysostosis with hormone resistance [5,64].

From the clinical standpoint, our study and the 2 recent studies indicate that skeletal dysplasia may be causally related to hormonal resistance through a signal transduction pathway. At one end of hormonal resistance lies PHP-1b, which is manifested as a resistance to hormones like PTH and TSH. However, the skeletal manifestations associated with

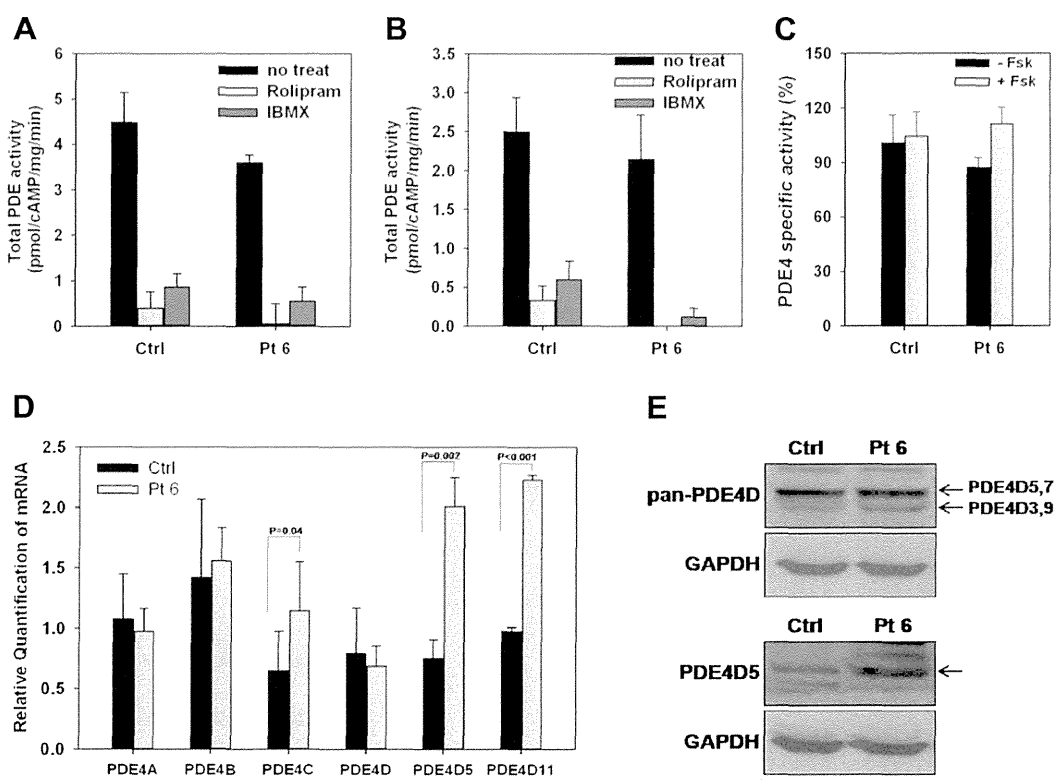


**Fig. 4.** Normal PDE4-specific activity in the acrodysostosis patient. EBV-transformed lymphocytes of control subject and patient 6 were harvested to measure the total PDE activity before (A) and after (B) Fsk stimulation (10 μM, 30 min) and also PDE4-specific activity (C). We measured the total cAMP-hydrolysing activity in the presence or absence of the pan-PDE inhibitor IBMX (100 μM), and in the presence of the PDE4-specific inhibitor rolipram (10 μM) to estimate the PDE4 fraction of the total PDE activity. In patient and control cells, total PDE and PDE4-specific activities were not different (means ± SD shown) (D). Because PDE4 activity levels were the same in the control subject and patient 6, we determined the expression of PDE4 and PDE4D isoform mRNAs in the patient. PDE4C isoform was increased in patient 6 in a statistically significant manner, and the expression of PDE4D isoforms was also increased; *$P < 0.05$, **$P < 0.005$ (E). PDE4D and PDE4D5 protein expressions. Overall PDE4D expression was similar in control and patient cells, but the expression of PDE4D5 isoform was slightly higher in patient cells.